Multiparticle interactions

1972 J. Phys. A: Gen. Phys. 5 27

(http://iopscience.iop.org/0022-3689/5/1/010)

J. Phys. A: Gen. Phys., Vol. 5, January 1972. Printed in Great Britain

Multiparticle interactions†

S J GOLDSACK

Department of Physics, Imperial College of Science and Technology, London, UK

MS received 12 August 1971

Abstract. A review is given of some recent work on the phenomenology of multiparticle interactions of hadrons. The treatment is in breadth rather than depth.

1. Introduction

When two hadrons collide at high energy, their interaction may lead to one of many final states. They may undergo elastic scattering, or they may react to form a two body or quasi-two body state. They are however much more likely to form a multiparticle final state. Figure 1 gives an approximate breakdown of the interaction cross section for K mesons on protons. At high energies the total cross section tends to a constant value of about 21 mb, and the elastic scattering is about 3·0 mb. Other quasi-two body states amount to about 1·5 mb at 10 GeV/c and appear still to be decreasing with energy. Since the elastic scattering is presumably mainly the diffractive shadow of the inelastic processes, it is clear that a description of the high energy interactions which ignores the multiparticle states is at best incomplete.

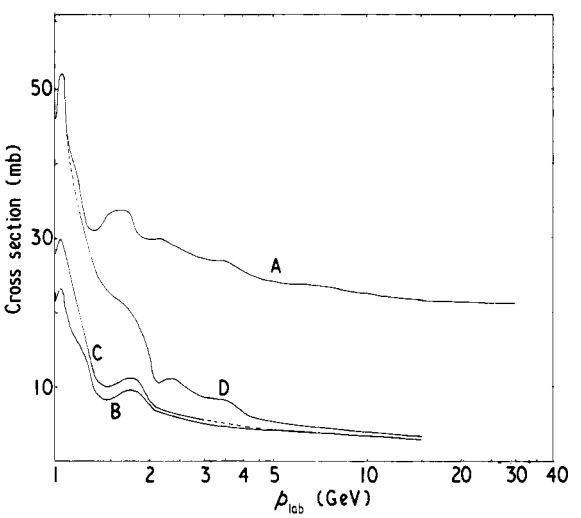

Figure 1. The K^-p interaction cross section and its decomposition into two-body and many body channels. Curve A is the total cross section; curve B is the elastic scattering cross section; curve C is elastic scattering including charge exchange; curve D is the total of all two-body and quasi-two-body processes. The difference between A and D represents the multiparticle processes. The data are from the HERA compilation (Flaminio *et al* 1970).

† Review talk given at the Lancaster Conference of the Institute of Physics, 5 April 1971.

In spite of this, many-particle states have received very little attention until the last year or two. There are several reasons for this. The many body problem is notoriously difficult, and the many body problem in strong interactions, themselves only poorly understood, is not a field of much interest to fundamental theorists.

On the experimental side, work has often been restricted to 'easy' topologies, either because of the limitation of measuring facilities, or because of the uncertainty of how to analyse the results anyway. However, in recent years a large amount of data have accumulated (though they are not often available in a useful form in the literature), and at the same time, perhaps because of the paucity of new fundamental ideas in theory, a number of theorists have given attention to the problem of multiparticle phenomenology. This has led to a certain amount of progress, which it is the purpose of this article to review.

The difficulty of the problem starts with the adequate description of the individual events. If there are k particles in the final state, each complete event is described by $(3k-4)$ variables. This is therefore the dimensionality of the phase space in which they can be mapped. Already, with only four particles, there are eight independent variables, and the results presented in the form of a few effective mass plots and four-momentum transfer distributions give a totally inadequate description of the whole system.

In practice, however we find experimentally that most of the available phase space is empty, a circumstance which greatly simplifies the analysis, since the distribution within the occupied parts of phase space can be studied with reasonable precision with the statistics presently available. In particular, it has been known for many years from cosmic ray studies, that the interactions always lead to low transverse momenta for all the particles† so that the region of phase space actually occupied is restricted to a 'shell' of rather constant thickness around the hypersurface defined by the constraints that all the transverse momenta are zero. This hypersurface can be referred to as longitudinal phase space, and has dimensionality $k-2$. We shall return to this in a later section.

The dynamics of our problem is contained in a transition amplitude T, giving the transition rate from the incoming two-particle state to some particular quantum state of the final multiparticle system. It is related to the cross sections which are the results of experiment by the well known 'Golden Rule'

$$\mathrm{d}\sigma = \frac{1}{\text{flux}} \int |T|^2 \, \mathrm{d}(\text{LIPS})$$

where we have written LIPS as shorthand for Lorenz-invariant phase space

$$\mathrm{d}(\text{LIPS}) = \prod_1^k \frac{\mathrm{d}^3 p_i}{2E_i} \delta^4(p_f - p_i).$$

The integration is carried out over all the variables of the problem except those with respect to which the distribution is required. If all the variables of integration are exhausted one gets the total cross section.

If the amplitude T were known for all final states, the problem of hadron physics would be solved. However we are far from being in that position; T is extremely

† Note, however, that this corresponds to the forward peaking of two body interactions. If at a later stage we wish to study the multiparticle states in regions with high transverse momenta, the problems will be correspondingly more difficult. In two-body processes, work is now being done to study large momentum transfers, where cross sections are several orders of magnitude smaller than in the forward peak. Multiparticle events are at present only being seriously studied in the equivalent of the forward peak.

complicated. For a k particle state it is a function of the $3k-4$ variables; we shall discuss some of its other properties later. The aim of experiment is to provide the information needed to guide us in determining these properties.

Unfortunately, the phase space integration is also very complicated. It is well known that for three or more particles, even the 'pure phase space' distributions, obtained by setting T equal to a constant, require numerical integration when three or more particles are involved. The difficulty of interpreting the experimentally observed distributions, is to unfold the effects of the dynamically trivial phase space. There are variables which are essentially 'flat' in a pure phase space distribution. Examples of these are most single-particle angular distributions and the density distribution on the Dalitz plot. However, these are the exceptions. Most quantities of dynamical interest have nontrivial phase space distributions, and it is part of the job of the phenomenologist to unfold the effects of the dynamics described by the amplitude.

An alternative approach is to construct a mathematical model for the amplitude; it is then possible to carry out the phase space integrations and so derive predictions for the actual measured distributions. One may possibly adjust a few parameters of the model, to obtain a 'fit' to the data. However the credibility of the model as a description of the real dynamics of the hadron interactions is greater, the fewer adjustable parameters are required.

In the following sections we shall discuss examples of both these approaches.

2. Multiplicity distributions

The simplest experiments to perform are those which study the charged particle multiplicity distributions, without regard to the nature of the particles produced, or to the neutral particles. Most workers agree that the distributions are well represented by some form of Poisson distribution, with a mean which increases slowly with incident energy. However there is some discussion as to what is distributed this way. A discussion of the various possibilities has been given by Wroblewski in his review talk at the Kiev Conference (Wroblewski 1970a) but probably the best formula is that of Wang (1969), who suggests that the distribution should be in pairs of produced particles. (In Wang's model there is local charge conservation, so the particles are assumed to be correlated in pairs.) The probability of k_c charged particles in the final state is therefore

$$P(k) = \frac{(\frac{1}{2}\langle k_c - 2\rangle)^{(k_c-2)/2}}{\{\frac{1}{2}(k_c-2)\}!}\exp(-\tfrac{1}{2}\langle k_c - 2\rangle).$$

The variable is $k_c - 2$ because we have two charged particles in the initial state.

Figure 2 shows the results of the Serpukhov photographic emulsion group for the mean multiplicity in π^- interactions. The figure is taken from Anzon *et al* (1970). The curves superimposed on the data are an $E^{0.35}$ law, consistent with the $E^{0.33}$ law predicted by Rotelli (1969) on the basis of a form of the statistical model, and the $\lg E$ dependence expected from a multi-Regge pole model (eg Chew and Pignotti 1968). These results seem to support the power law, but the difference is not great. Figure 3 shows the results of Jones *et al* (1970) who have carried out a cosmic ray experiment, using a large liquid hydrogen target, with a total absorption calorimeter to determine the energy. This will give mainly proton interactions, and the data include laboratory energies an order of magnitude higher than the Serpukhov results. Here the experiment

seems to support the lg E dependence. Possible objections can be raised to the experimental techniques of both groups, so a final answer may have to await experiments at the CERN intersecting storage rings, or at the new accelerators. In the mean time it is the author's opinion that the results of Jones *et al* would have to be too far in error for the power law to be given much credence.

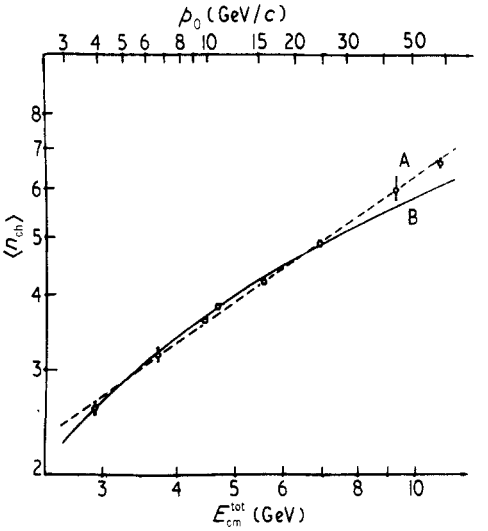

Figure 2. Average prong number $\langle n_{ch} \rangle$ in π p interactions as a function of the centre of mass energy. The data are from the Serpukhov emulsion group (Anzon *et al* 1970). Curve A, $\langle n_{ch} \rangle \simeq E_0^{0.35}$; curve B $\langle n_{ch} \rangle \simeq \lg E_0$.

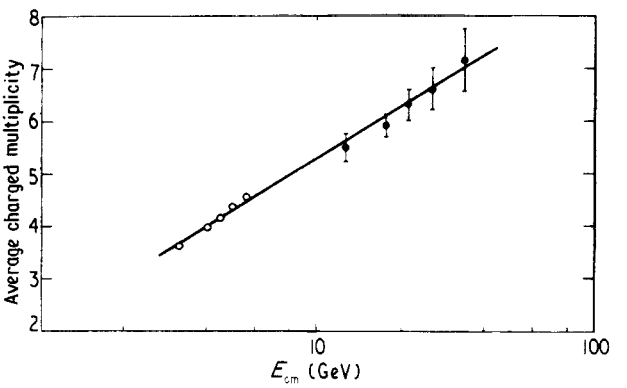

Figure 3. Average prong number in pp interactions. Data are from the Echo-Lake cosmic ray experiment (Jones 1970). The curve is the lg s dependence predicted by a multiperipheral model.

3. Channel cross sections

After the multiplicity distributions, the most immediately accessible features of the multiparticle interactions are the individual channel reaction cross sections. The lower curves of figure 4 show the total cross sections for the reactions $\pi^+ p \rightarrow p\pi^+\pi^+\pi^-$ and

$\pi^- p \to p\pi^-\pi^+\pi^-\pi^0$. These are very typical of all the cases, showing a rapid rise from threshold, followed by a fall away at high energies. It is apparent that the rise from threshold is due to the opening up of the available phase space volume. However, for a k particle final state, the phase space volume behaves asymptotically like s^{k-2}†, so that it continues to increase at high energies. The fall off must therefore be a property of the amplitude. To separate the two effects we can divide the cross section by the total phase space volume. This was first done by Muirhead and Poppleton (1969) for the case of antiproton annihilations. It was carried out systematically for many different reactions by Hofmokl and Wroblewski (1970, figure 4 is reproduced from their paper).

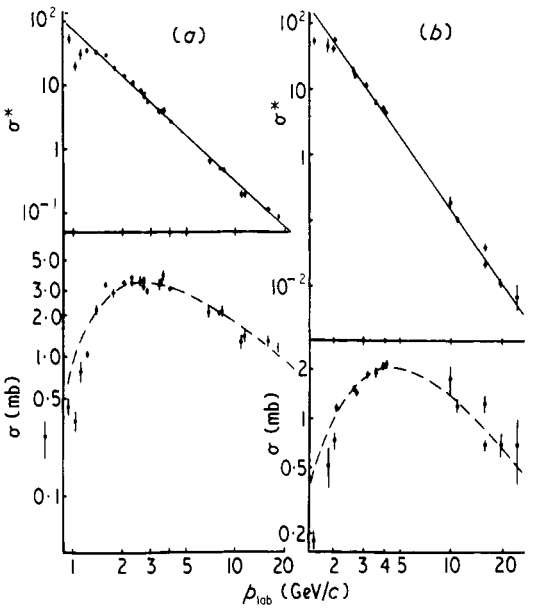

Figure 4. Total cross sections for (*a*) $\pi^+ p \to p\pi^+\pi^+\pi^-$ and (*b*) $\pi^- p \to p\pi^+\pi^+\pi^-\pi^0$. The lower curves are the raw data; the upper curves are after division by total phase space. Curves are from Hofmokl and Wroblewski (1970).

The upper curves show the cross sections σ^* adjusted for phase space in this way. The results are very beautiful straight lines on the lg plot, showing that a relation of the type $\sigma^* \propto S^{-n}$ is a very good parameterization of the data. The value of n was obtained for each of the processes, and figure 5 shows n as a function of multiplicity, for a series of different types of reaction.

The result illustrated in figure 5 is most striking; for each class of reaction the value of n increases by exactly one for each increase in multiplicity. This is clearly telling us something quite simple and important. In fact there is little doubt what it is. As we have already seen the interactions do not fill phase space; rather, they are restricted to that shell around the longitudinal phase space which we have discussed above. This shell occupies a smaller and smaller fraction of the total phase space as the energy increases, and instead of increasing without limit at high energies, it tends, approximately, to a constant‡. Of course the reason for the restriction to low transverse

† Throughout this article s has its usual meaning of the squared energy in the centre of mass frame.

‡ Actually it increases logarithmically.

momenta is itself a property of the amplitude T. However, it is so universal, and appears to be a property so independent of all other properties of the amplitude that it seems not unreasonable to factor it out along with the phase space, dividing by the volume, not of total phase space, but of longitudinal phase space, represented by LIPS/s^{k-2}, which tends to a constant at high energy.

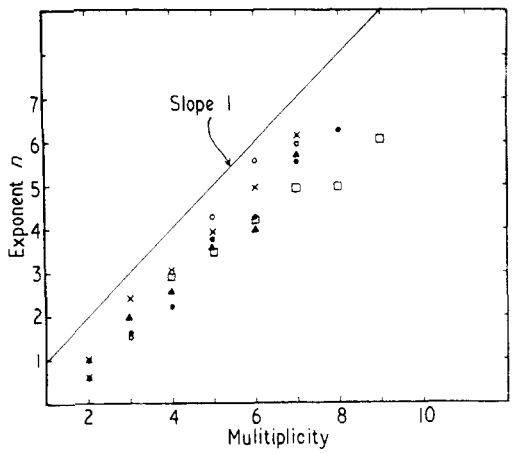

Figure 5. Logarithmic slope n of the cross sections corrected for phase space, as a function of multiplicity (from Wroblewski 1970a). ● πp; ○ pp; × Kp; ▲ γp; □ p̄p → pions.

This was done by Hansen *et al* (1970), some of whose results are reproduced in figure 6. The way in which different multiplicities give the same slope is most convincing, and even more striking is the comparison with the slopes of the corresponding two-body processes. To a first approximation, at least, these slopes are the same, ranging from about two where nonstrange meson exchange is possible, to about four in reactions where baryon exchange is required. There is little doubt that this behaviour is a strong indication of multi-Regge behaviour of the amplitude at high energies.

These results are summarized in table 1, which is taken from the paper of Hansen *et al* (1970).

Table 1. Logarithmic slope parameter n for many body processes compared with the value for corresponding two-body processes (from Hansen *et al* 1970)

Two-body		Many-body			
Exchange	n	Reaction	Exchange		n_A
			Dominant	Secondary	
Pomeron	0·2				
$S = 0$ meson	2	$(\pi, K, p) + p \rightarrow (\pi, K, N) + N +$ pions	$S = 0$ meson	Pomeron, baryon	2
$S = 1$ meson	2·5	$K^- p \rightarrow \Lambda +$ pions	$S = 1$ meson	Baryon	3
Baryon	4	$K^- p \rightarrow \Xi^- + K +$ pions	Baryon	$S = 1$ meson	4

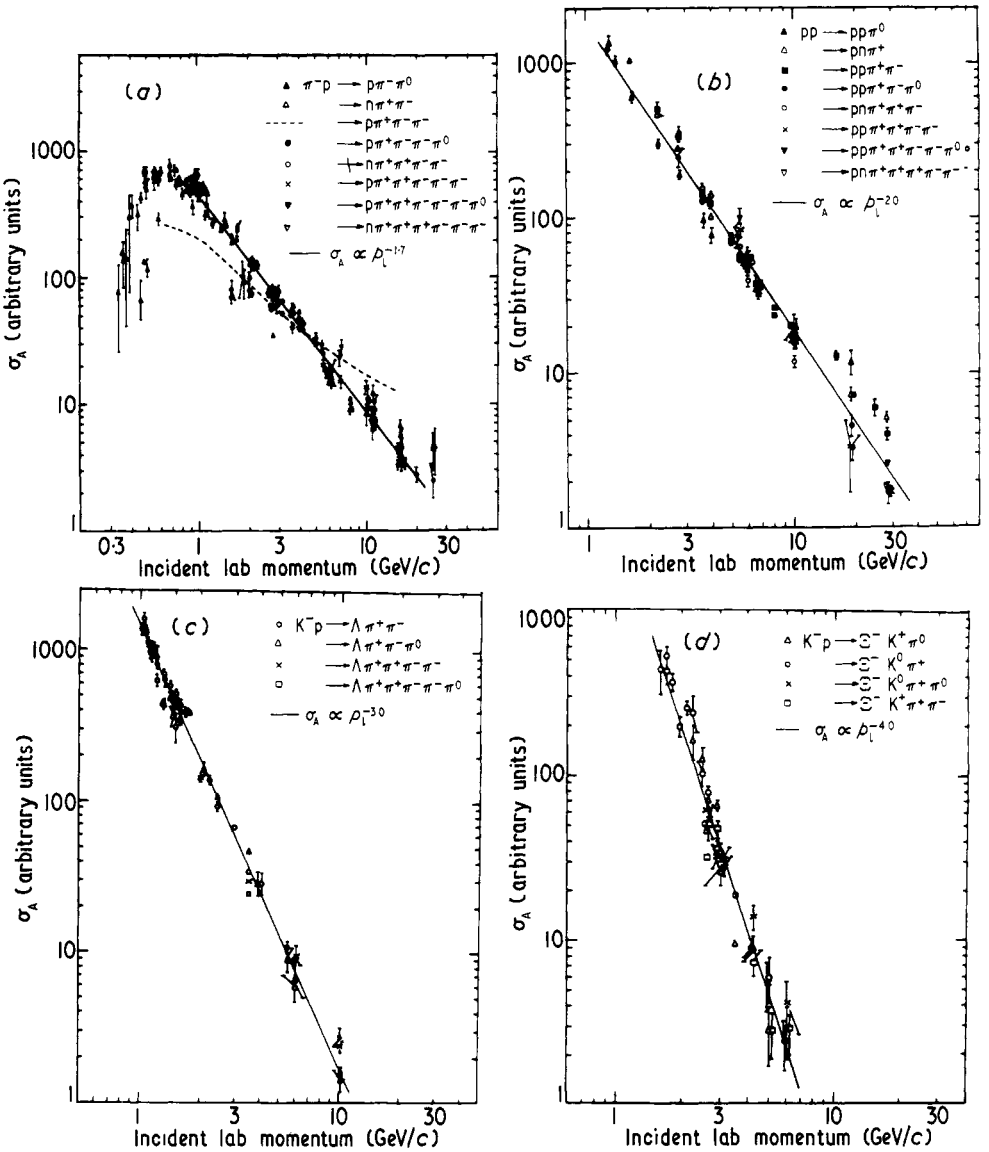

Figure 6. Total cross sections corrected for 'longitudinal phase space' for reactions of four different classes (from Hansen *et al* 1970). (*a*) $\pi^- p \rightarrow p + \text{pions}$; (*b*) $pp \rightarrow N + N + \text{pions}$; (*c*) $K^- p \rightarrow \Lambda + \text{pions}$; (*d*) $K^- p \rightarrow \Xi^- K + \text{pions}$.

4. Topological cross sections

It is interesting to note that, unlike the cross sections for individual completely defined final states, the cross sections for events selected only by their number of charged prongs (irrespective of the number of neutral particles associated) rise from threshold to a maximum, after which they remain almost constant (figure 7). This seems to be characteristic of the so called 'inclusive' reactions, about which we shall say more later.

Wroblewski (1970b) has pointed out that the data seem to suggest a simple regularity. If one plots the cross section for k particle states as a function of the mean centre of mass energy per particle, the cross sections seem to lie on a series of curves which differ only by a factor of two in cross section for each increase in multiplicity. That is

$$\sigma_K\left(\frac{E^*}{k}\right) = 2\sigma_{K+1}\left(\frac{E^*}{k+1}\right)$$

where the brackets imply functional dependence. This is illustrated in figure 8.

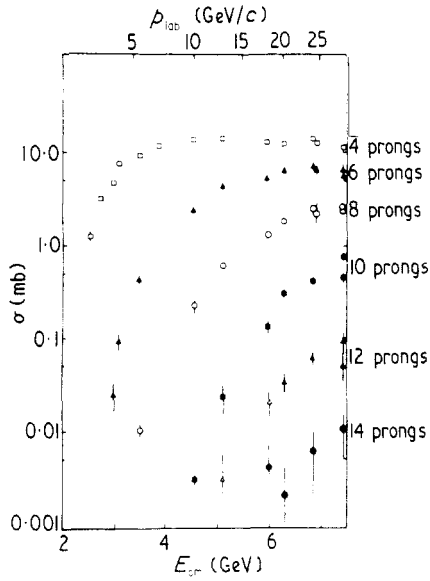

Figure 7. Topological cross sections, as a function of the beam momentum (top scale) and of the centre of mass energy (bottom scale).

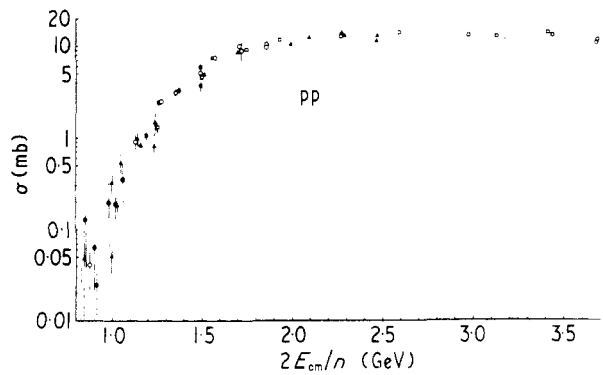

Figure 8. Illustrates Wroblewski's proposed simple regularity (see text). □ σ_4; ▲ $\sigma_6 \times 2$; ○ $\sigma_8 \times 4$; ■ $\sigma_{10} \times 8$; ▲ $\sigma_{12} \times 16$; ● $\sigma_{14} \times 32$.

Taken with a constant asymptotic cross section this would imply, contrary to experiment, a constant mean multiplicity at high energies. Moreover, the preliminary results from Serpukhov (Anzon *et al* 1970) show that the six-prong cross section is

higher than the four-prong in the 50 GeV region (see figure 9). It follows that the constancy of cross sections can only be approximate.

Moreover, if the mean multiplicity is increasing with energy, while the total cross section remains constant, individual channel cross sections must decrease slowly. Wroblewski's conjecture is, moreover, inconsistent with the Poisson distribution mentioned in § 3.

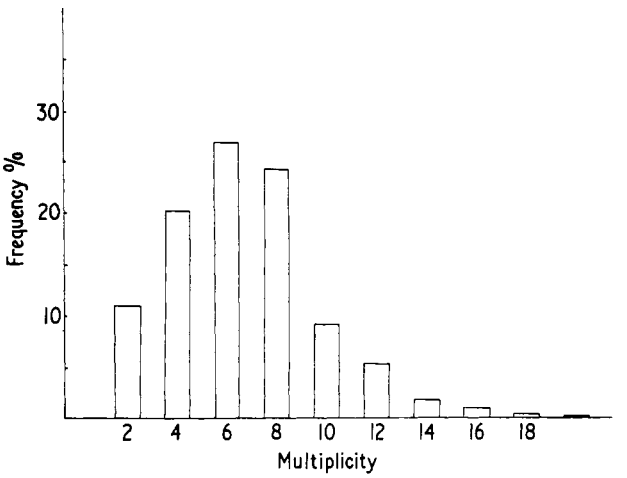

Figure 9. Multiplicity distribution for π^-p interactions at 60 GeV. The data are from Anzon *et al* (1970) and are inferred from interactions in emulsions.

5. *F(t)* distributions

While on the subject of 'dividing out' phase space effects, we should mention the work of the ABBCCHW collaboration (Honecker *et al* 1971), who have studied the distribution of the four-momentum transfer t for the interactions of the type $\pi^-\text{p} \rightarrow$ nucleon + pions. For each multiplicity they have evaluated

$$F(t) = \frac{\mathrm{d}\sigma/\mathrm{d}t}{\mathrm{d}\sigma/\mathrm{d}t\ (\text{phase space})}$$

where $\mathrm{d}\sigma/\mathrm{d}t$ (phase space) is the calculated shape of the differential cross section with $|T|^2 = 1$. This function should give the dependence of the square of the matrix element on t, averaged over all the other variables. The results shown in figure 10 show that the distribution is not very dependent on multiplicity and that each one is close in shape to the curve $1/(m_\pi^2 - t)$ which is the pion propagator. It is not clear at present whether this must be regarded as having any fundamental significance.

6. Resonance production

In the previous sections each final state was treated independently of the mechanism by which it was produced. In practice a very important feature of all such processes is the resonance nature of the interactions between pairs or larger groups of the final

state particles. This being so, one may wonder whether there is any sense in combining all these processes in the above analysis. Should, say, a five particle state with a resonance not be classed as a quasi-four-body state? It is one of the nice features of the asymptotic behaviour described above that it actually does not matter, since the energy dependence at high energy is the same. This does imply, however, that the resonance fractions do not decrease with energy, since we should have the same energy dependence for, say, the process $\pi p \rightarrow \rho\pi p$ as for the process $\pi p \rightarrow \pi\pi\pi p$ of which the first forms a subset.

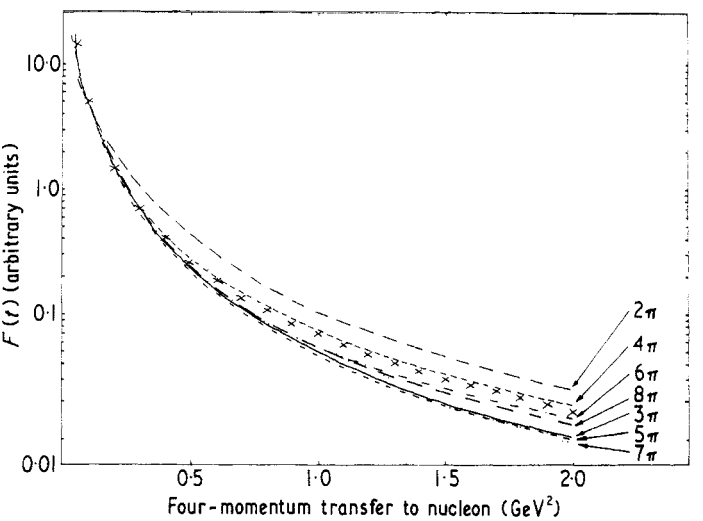

Figure 10. Distributions of the four-momentum transfer from proton to nucleon in reactions $\pi + p \rightarrow$ nucleon $+ n$ (pions), after dividing by the expected phase space distribution (from Honecker *et al* 1971). The crosses represent the pion propagator.

Indications are that this is at least approximately true. Wroblewski, in his talk at the Kiev Conference, gave a compilation of the fraction of ρ mesons and of Δ in pi–p interactions over a wide range of incident momentum. Though the errors are large, there is no indication that there is a trend upwards or downwards. Similar results have been found for $k^- p$ interactions (Goldsack 1971)†. Table 2 shows the fractions of K^{*-}, ρ^0 and Δ^{++} found in the channel $k^- p - k^0 p \pi^+ \pi^- \pi^-$ at 6 GeV/c and 10 GeV/c. There are several interesting features. First, one notes the extremely high proportion of resonances, more than one per event on the average. Secondly, there seems little change in the fractions between the two energies. Lastly, it may be relevant to point out that the fraction of K^* when Δ is produced, is about the same as the fraction of K^* in the whole sample. The same is true of the fraction of Δ when K^* is produced. (The fraction of ρ when K^* is produced is less than in the whole data but this is to be expected, since each requires a π^-.) Thus it seems that the simultaneous $K^*\Delta$ production, although a substantial contribution to the channel, does not represent any cooperative behaviour between the two resonances.

There is room for much further work of this type. At present there is too little uniformity in the methods of fitting the resonance fractions to allow much confidence in comparison between the work of different groups, and there is in any case little work reported in the literature.

† Also ABCLV collaboration, submitted to the Amsterdam International Conference, June 1971.

Table 2. Resonance production in $K^-p \to K^0p\pi^+\pi^-\pi^-$ at 6 GeV/c and 10 GeV/c

Final states	Resonance fractions %	
	6 GeV/c	10 GeV/c
$\Delta^{++}K^0\pi^-\pi^-$	13 ± 4	15 ± 1
$pK^*\pi^-\pi^+$	25 ± 6	21 ± 3
$pK\rho^0\pi^-$	25 ± 5	31 ± 2
$\Delta^{++}K^*\pi^-$	20 ± 5	15 ± 4
$pK^{*-}\rho^0$	17 ± 6	19 ± 2
$pK^-\pi^+\pi^-\pi^-$	0 ± 2	0 ± 2
Total K^*	67 ± 8	55 ± 4
Total Δ	33 ± 7	34 ± 4
Total ρ^0	42 ± 8	50 ± 4
K^* fraction of Δ	60 ± 10	56 ± 6
Δ fraction of K^*	30 ± 7	27 ± 6
K^* fraction of ρ^0	40 ± 10	38 ± 3

7. The importance of the pomeron

The results presented in § 3 show how each individual production process decreases as a power of the squared energy. At the same time the elastic scattering cross section is substantially constant. This is interpreted as due to the diffractive nature of the elastic scattering, which in Regge theory is parameterized by the exchange of a 'pomeron'. That diffractive processes can also give rise to dissociation of the colliding particles has been appreciated for some time. It is perhaps most clearly seen by consideration of the so called Deck effect, illustrated in figure 11. One incident particle dissociates

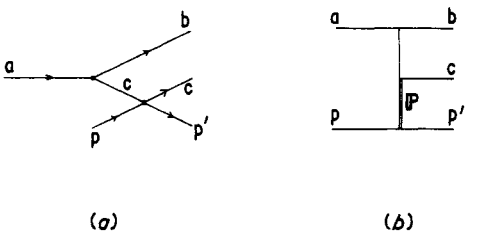

Figure 11. The Deck effect. (*a*) Illustrates the effect in a pictorial manner; (*b*) the equivalent multiperipheral graph, where the scattering of the particle c is assumed to be by pomeron exchange.

virtually into a pair of intermediate particles to which it is strongly coupled. While in this state one of the virtual particles undergoes scattering at the target, generating a real three-particle final state. At high enough energies this scattering will also mainly be diffractive. Such processes are of course inelastic, insofar as they scatter particles out of the incoming channel. As such they contribute to the absorption of which the elastic scattering is a shadow. However these simple Deck processes must themselves be a shadow of still more deeply inelastic processes. The cross section for diffractive

processes is not expected to decrease rapidly with energy, so that their contribution must become increasingly important as the energy increases. This emphasis on the Deck-like processes, which gives a rather pictorial view of the diffraction dissociation process, should not hide the fact that resonant states can also be excited by pomeron exchange.

At the energies currently available for study in a systematic way with the bubble chamber, the effects of the pomeron are certainly not dominant except in certain special channels. This is evident since processes to which pomeron exchange must contribute at high energy are still seen to be decreasing at the highest energies presently accessible. However, certain specially favoured processes do seem to show the diffractive effects at moderate energies. In particular, the four body final states with incident pions, associated with the production of the A_1 meson, have cross sections decreasing rather slowly with energy, as seen in figure 6. Later we shall see that, by examining the structure of certain other processes sufficiently closely, evidence is found that the pomeron is contributing even there.

8. Longitudinal phase space analysis

It has been emphasized above that the most striking single property of the amplitude for any process is its peripherality. All particles share a cut-off in the transverse momentum with a fairly constant range, so that the events are confined to that shell within the phase space which was referred to in § 1 as the longitudinal phase space (LPS). It is therefore of interest to display the data in a way which shows how the events are distributed with respect to the remaining variables, which define their position within the LPS. A convenient way of doing this has been provided by Van Hove (1969). We shall see that this provides us with a means of finding the contributions of diffractive events.

Apart from the transverse momentum, each separate particle i is characterized by the longitudinal component of its momentum q_i†. The position of each event in LPS is therefore specified by the set of quantities q_i. However, these are not independent quantities; if the q_i are measured in the centre of mass frame, they are constrained by the momentum conservation to satisfy $\Sigma q_i = 0$. It is therefore possible to display the distributions of the values for three particles on a two dimensional scatter plot, where the longitudinal momenta are measured with respect to a set of three axes at 120° to each other as in figure 12. It is easy to see that the momentum conservation is automatically satisfied for any point in the plane. If we can neglect the energy associated with the transverse motion, there is the additional constraint $\Sigma(q_i^2+m_i^2)^{1/2} = s^{1/2}$. This defines the kinematic limit for the plot, and in practice all points cluster close to the boundary. Some examples are shown in figure 13 (Bartsch *et al* 1970c). The points now form an essentially one dimensional distribution, and it is therefore possible to display them as a histogram in terms of the angle θ which is also defined in figure 12.

At very high energies a multiperipheral model predicts the ordering of the longitudinal momenta according to the order of the particles in the corresponding Feynman ladder graph; at more moderate energies one may expect this to be broadly true, though the boundaries may be less sharply defined. Figure 12 also shows the regions of the LPS plot which may be expected to be populated by events produced by the mechanisms indicated. In particular there is a region between 90° and 120° which corresponds to the graph in which the target nucleon and the created pion are at one vertex, while the

† q has the same meaning as $p_{\parallel}$ used in § 11.

incident particle is at the other. This is the region where one would expect to find events created by the diffraction dissociation of the proton. If this process is giving a large contribution to the single meson production one may expect to find a large peak in the distribution in this neighbourhood, followed by a sharp drop near 120° since the diffractive process does not readily throw mesons into the 'wrong' hemisphere. Note that dissociation of the beam particle would lead to a similar peak near 150° but diffraction dissociation of a pseudoscalar meson into two other similar mesons is forbidden by spin and parity conservation. This behaviour is clearly visible in figure 14. (Dissociation of the pion and the proton are both possible in the pωπ channel, and figure 13(*d*) shows that both processes seem to be occurring.)

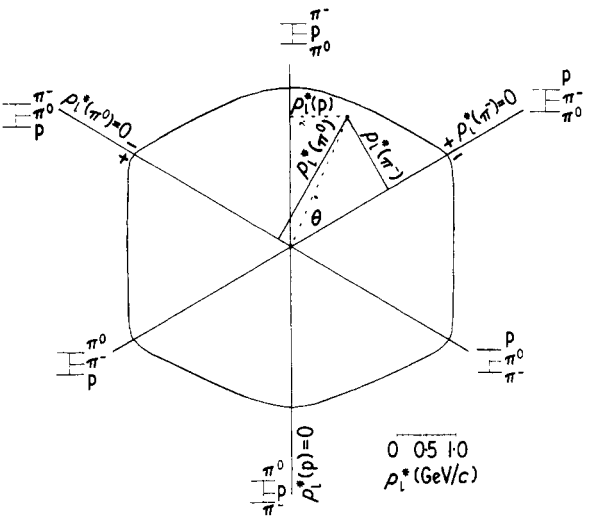

Figure 12. The Van Hove longitudinal phase space plot, drawn here for the case $\pi^+ p \to \pi^- \pi^0 p$ at 16 GeV/*c*, and showing the definition of the angle θ. Inset are the multiperipheral graphs which can be expected to contribute in the different regions of the plot.

Though we have already seen that the cross section for single pion production appears to be falling rapidly with energy according to the s^{-n} rule, one can still see if there is a subclass of events which persists to high energy by evaluating the parameter n for different regions of the LPS angle. Such an analysis, performed by Rinaudo *et al* (1971) is shown in figure 15. It shows clearly that, in the diffractive region, n is indeed close to zero, though it is large elsewhere. This shows that in these channels the effects of pomeron exchange are just below the surface, and will presumably show as a flattening of the total cross section as we increase the energy still further. Recent analyses of the single pion production by k mesons described in § 17 have used a multiparticle Veneziano amplitude to describe the nondiffractive part of the data, and estimated quantitatively the fraction of the cross section which is diffractive. The results vary between 25 % to 50 % in different three-body channels around 10 GeV/*c*.

The generalization of the Van Hove hexagon plot to four bodies has also been given by Van Hove; there are now three independent longitudinal momenta, so the four values can be plotted in three dimensional space with axes referred to a set of four planes intersecting at a point. The equivalent of the hexagon, which provides the kinematic limit for the plot, is a cube–octohedron, a 14-sided semiregular solid figure

illustrated in figure 16. Again the events cluster in practice close to their kinematic limit, because of the low transverse momenta. It is therefore possible to study the complete distribution as a two dimensional scatter plot in a pair of polar angles corresponding to the Van Hove angle. However, that presentation is rather remote from the physical processes involved, so that its significance is difficult to appreciate. In figure 17 is shown an example where the points have been projected onto the surface of the cube–octohedron, which has then been unfolded to make a two dimensional distribution. However, in many cases there are well defined 'leading' particles. For example, the proton is nearly always backwards, and the kaon forwards in reactions $k^{\pm}p \rightarrow k^{\pm}p\pi^{+}\pi^{-}$.

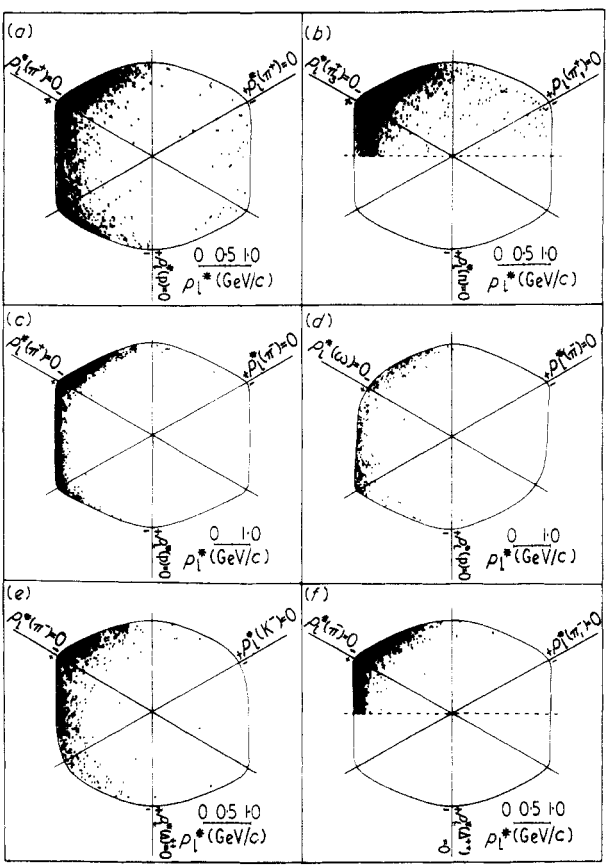

Figure 13. Examples of the longitudinal phase space plot, showing how events cluster near the kinematic boundary, in an essentially one dimensional distribution. (*a*) $\pi^{+}p \rightarrow p\pi^{+}\pi^{0}$, at 8 GeV/*c*, 2168 events; (*b*) $\pi^{+}p \rightarrow n\pi^{+}\pi^{+}$, at 8 GeV/*c*, 1825 events; (*c*) $\pi^{-}p \rightarrow p\pi^{-}\pi^{0}$, at 16 GeV/*c*, 903 events; (*d*) $\pi^{-}p \rightarrow p\pi^{-}\omega$, at 16 GeV/*c*, 299 events; (*e*) $K^{-}p \rightarrow \Delta^{++}K^{-}\pi^{-}$, at 10 GeV/*c*, 683 events; (*f*) $\pi^{-}p \rightarrow \Delta^{++}\pi^{-}\pi^{-}$, at 16 GeV/*c*, 1308 events (Bartsch *et al* 1970c).

In this case only four adjacent faces of the cube–octohedron are populated, and a neater presentation is that given by Kittel *et al* (1970) where events are described by two longitudinal momenta, those of the produced (ie nonleading) particles. However, instead of the longitudinal momenta themselves, one plots the reduced variables $x_i = 2q_i/\Sigma_i|q_i|$. At high energy Σq_i approaches $s^{1/2}$, so that in this limit these variables

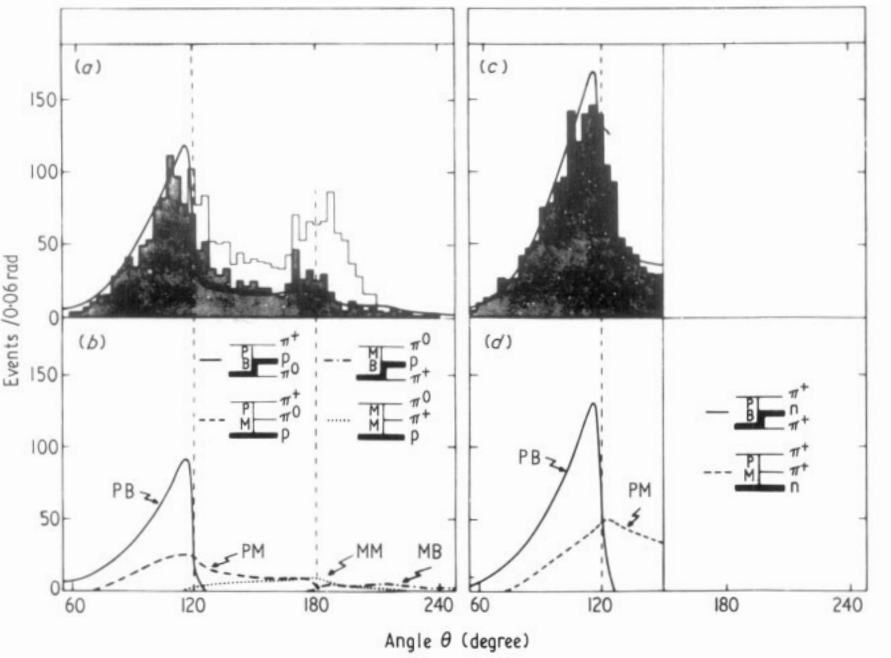

Figure 14. Examples of the LPS analysis (Bartsch *et al* 1970c). Showing the sharp drop near 120° associated with dissociation of the nucleon. The curves are the predictions of the CLA model (§ 15). The lower curves show how these are composed of contributions from different multiperipheral processes. The baryon exchange is undoubtedly exaggerated in this work by the existence of resonances which are neglected in the CLA model. P stands for pomeron, B for baryon and M for meson in labelling the exchange. (*a*) and (*b*) $\pi^+ p \rightarrow p\pi^+\pi^0$, at 8 GeV/*c*, 2168 events, ■ ρ and Δ^{++} out, 1456 events, —— CLA model; (*c*) and (*d*) $\pi^+ p \rightarrow n\pi^+\pi^+$, at 8 GeV/*c*, 1825 events, —— CLA model.

are equivalent to the variables introduced by Feynman to describe single particle distributions (see § 11). The variables used here have the advantage that the approximate constraint of conservation of energy is replaced by the exact constraint $\Sigma|x_i| = 2$, so that the points lie in the surface, not just below it. A scatter plot of x_1 against x_2 is equivalent to the four corresponding faces of the cube–octohedron, and figure 18 shows how events may be expected to be distributed if they are created according to the mechanisms indicated. In particular, the events due to the diffraction dissociation of the beam and target respectively into three particles are to be found in the upper right and lower left quadrants of the plot. The results of this analysis for negative pion interactions at 11 and 16 GeV/*c* are shown in figure 19, due to Kittel *et al* (1971). Here x_1 and x_2 refer to the longitudinal momenta of the π^+ and the produced π^- respectively. In figure 20 the value of the exponent n is shown for different areas of the plot. Again we find that the cross section is nearly constant in the regions where diffraction dissociation is to be expected. We can discern regions corresponding to the dissociations $\pi^- \rightarrow \pi^-\pi^+\pi^-$ and $p \rightarrow p\pi^+\pi^-$.

9. Isotopic spin analysis

In general the isotopic spin analysis of many-particle states involves many more amplitudes than there are accessible experimental channels, so that no valuable decomposition can be achieved. However, in the case of positive pion interactions with protons we

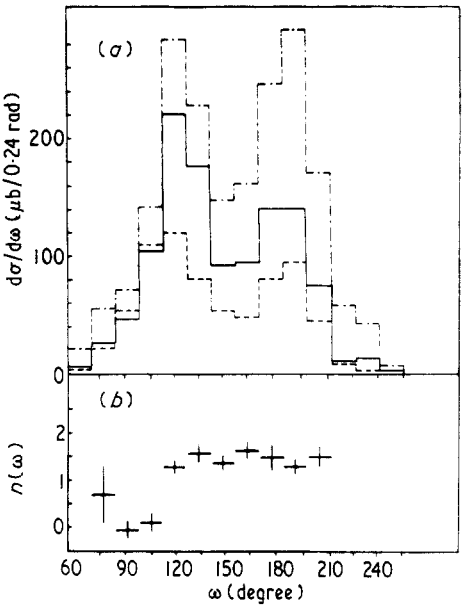

Figure 15. (*a*) Distributions in the Van Hove angle for $\pi p \rightarrow \pi\pi p$ at 4 GeV/*c* (chain curve, 977 eV), 5 GeV/*c* (full curve, 2648 eV) and 8 GeV/*c* (broken curve, 2134 eV), and (*b*) the value of the logarithmic slope parameter *n* at each angle. Data are from the Bonn, Durham, Nijmegen, Paris EP, Torino collaboration (Rinaudo *et al* 1971).

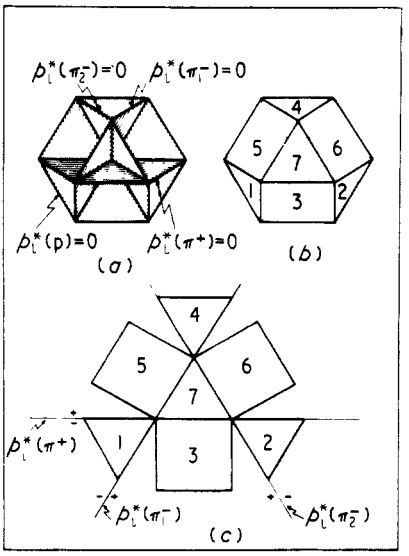

Figure 16. The cube–octohadron plot; the generalization to four-particle final states of the Van Hove hexagon. $\pi^- p \rightarrow p\pi^+\pi_1^-\pi_2^-$, at 16 GeV/*c*.

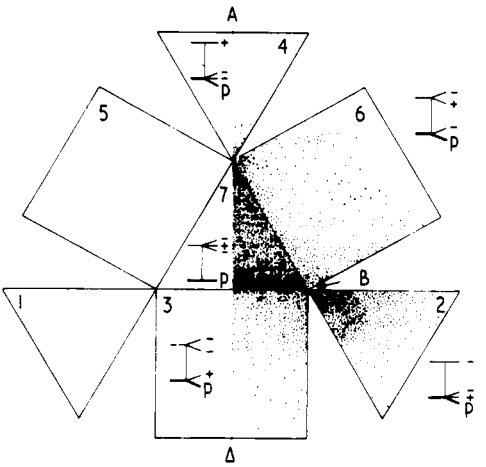

Figure 17. Example of the application of the cube–octohadron plot for $\pi^- p \to \pi^- \pi^+ \pi^- p$ at 16 GeV/c (Bartsch *et al* 1970).

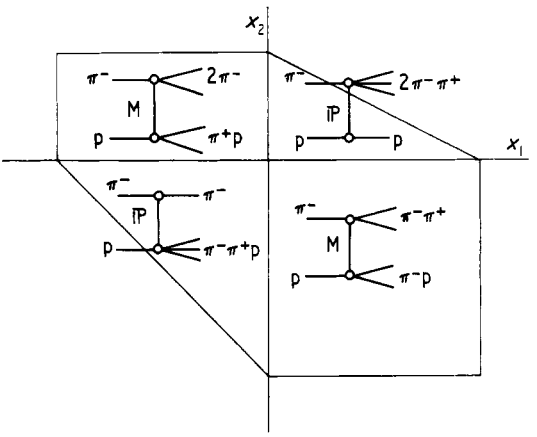

Figure 18. Modified LPS plot for four particles. x_1 and x_2 are the reduced longitudinal momentum variables for the produced particles.

have a pure $I = \frac{3}{2}$ system, and for three-body states there are three accessible channels, which are sufficient to fix the two amplitudes and their relative phase. The way in which the amplitudes can be chosen is not unique but it is of special interest to choose states in which the nucleon and produced pion form a system of isotopic spin $\frac{1}{2}$ and $\frac{3}{2}$ respectively. Diffraction dissociation can be expected to contribute only to the former. The full analysis in this way for π^+ at 4, 5, 8 and 16 GeV/c has been presented by Boesebeck *et al* (1971). In figure 21 this analysis is combined with the LPS analysis. We notice that the parameter n is close to zero for the system with isotopic spin $\frac{1}{2}$ and near the angle of 90° where diffractive effects are expected to be most important. The I spin $\frac{3}{2}$ does not show this feature, so that the cross section associated with nonzero isospin exchange has no energy independent component. At still higher energy we can expect this channel to become dominated by diffractive effects, giving a pure $I = \frac{1}{2}$ nucleon–pion system.

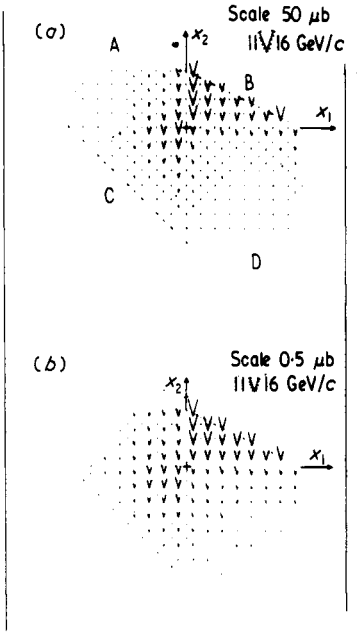

Figure 19. Example of the application of the modified LPS plot to the case $\pi^-p \to \pi^-\pi^-\pi^+p$ at 11 and 16 GeV/c. In each bin of the plot, the cross section has been indicated by the length of the line. (*a*) Number of events unweighted; (*b*) number of events weighted. The energies are distinguished by sloping the 11 GeV/c value to the left and the 16 GeV/c value to the right. In the lower plot the events have been weighted to allow for the phase space probability of each event (see Kittel *et al* 1970).

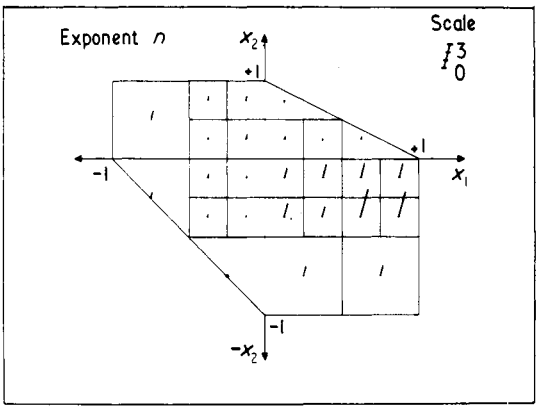

Figure 20. The logarithmic slope parameter n in different regions of the LPS plot for the case $\pi^-p \to \pi^-\pi^-\pi^+p$ at 11 and 16 GeV/c. The small value of n in the upper right and lower left quadrants indicates the dominance of the diffractive mechanism in the regions.

10. Summary on diffractive effects

We can conclude this section on the diffractive effects or pomeron exchange processes by remarking that at energies at present being studied, the obvious effects amount to about 1·5–2 mb, mainly in the four particle final states. It is, however, uncertain how

much of the multineutral final states, which are not measured in the bubble chamber experiments, may have their origin in the pomeron exchange. On looking more closely it is possible to see that several other processes are likely to become diffraction dominated at higher energies, and it is possible, though by no means proved, that these processes may eventually dominate every channel.

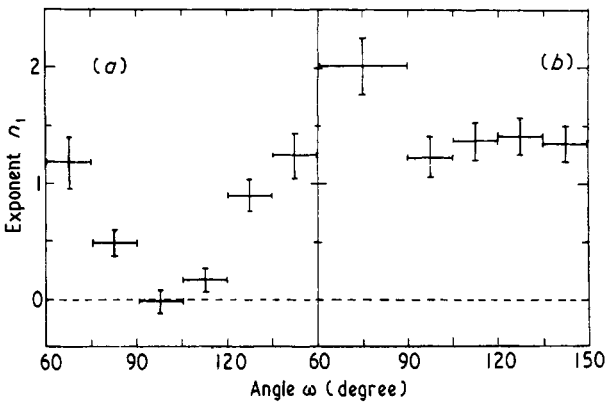

Figure 21. The logarithmic slope parameter n as a function of the Van Hove angle for the processes $\pi^+ p \to \pi^+(\pi N)^+$ at 4, 5, 8 and 16 GeV/c where contributions for (*a*) $\frac{1}{2}$ and (*b*) $\frac{3}{2}$ isospin for the dissociated nucleon have been separated.

11. Inclusive interactions

Every few years there comes a new idea which provides a novel way of looking at data to cast fresh light on the subject. A paper by Feynman (1969) has given rise to a wave of activity in the analysis of data, the re-analysis of old data, and the construction of new experiments. This new growth industry is the study of interactions from what Feynman calls the inclusive points of view.

So far multiparticle states have been mainly studied by isolating samples of events with the same well defined final state (Feynman calls this an exclusive interaction) and attempting to understand its dynamics in isolation from other channels. Now as we have seen, each such channel has a cross section which is a small and rapidly varying fraction of the total cross section. While each final state goes through these rapid variations however, the total cross section is a smooth function of the energy, apparently almost constant at high energies. It is clear that in some degree the variations of individual channels are due to competition from other processes, and that in some ways the description of the whole may be simpler than its parts. Feynman therefore suggests studying the momentum distribution of the individual particles irrespective of the mechanism by which they are created (ie summed over all the different final states). This is of course particularly attractive to the experimenter, since the bubble chamber man can now incorporate all his unfitted events, and the counter physicist has a new outlet for his one-armed spectrometer. This accounts for the wave of activity†.

† A further boost for the study of reactions from an inclusive point of view has been given by the demonstration by Mueller (1970) that the cross section for a reaction $a+b \to c+$ anything can be related by unitarity to the elastic three-particle scattering amplitude, $a+b+\bar{c} \to a+b+\bar{c}$ just as the two-body total cross section $a+b \to$ anything can be related to the elastic scattering $a+b \to a+b$. This leads to a new type of Regge phenomenology which may prove to be of great importance (see Chan Hong-Mo *et al* 1971).

Based on simple arguments of a partly intuitive nature, Feynman suggested that such a reaction would have a constant total cross section at high energies, and that the single-particle momentum spectrum could be written†

$$\frac{d^2\sigma}{dp_{ll}\,dp_t^2} = \frac{1}{E} f(p_{ll}, p_t, s)$$

where f is an invariant function, since $dp_{ll}\,dp_t^2/E$ is the Lorentz-invariant phase space element. It was suggested by Feynman that at high energies this function could be expected to be dependent on p_{ll} and s only through the ratio $x = 2p_{ll}/s^{1/2}$. In this sense the momentum spectra should 'scale', and be given by the universal function $f(p_t, x)$. The first tests of this idea have appeared in the literature in the last few months, and no doubt many more will follow.

This conjecture of Feynman is closely related to another due to Beneke *et al* (1969) and usually referred to as 'limiting fragmentation'. Here it is argued that the centre of mass frame is not a preferred frame of reference for high energy collisions, since the particles certainly do not 'stop on each other'. It is assumed that most of the particles are produced as fragmentation products of either the incident or the target particle, and that the fraction of pions produced slow in the centre of mass (so called pionization) would tend to zero at very high energy. In this case the produced particle momentum distribution would tend to a limiting form in the rest frame of the fragmenting particle. In fact as we shall see there is no evidence at present that the produced particles separate into two groups associated with the beam and target particles at the energies at present being studied.

Figure 22 shows the distributions in the variable x, integrated over the transverse momentum, of the pions from the reactions $\pi^- p \to \pi^+ +$anything and $\pi^- p \to \pi^- +$anything obtained by Biswas *et al* (1971) in an experiment at 18·5 GeV/c. The distributions are also shown separated according to the number of charged prongs. These are logarithmic histograms, and fit very well to an exponential distribution on each side of zero. This sharp peaking in the cross section is associated with the $1/E$ factor in the phase space volume element, which makes the phase space element large when the energy is small. This kinematic effect, which is most important for pions, because of their small mass, can be removed by weighting the events according to the energy when forming the histogram. This is equivalent to plotting

$$\int E \frac{d^2\sigma}{dp_t^2\,dp_{ll}}\,dp_t^2.$$

Alternatively the distribution in the rapidity variable $y = \frac{1}{2}\lg(E+p_{ll})/(E-p_{ll})$ can be used‡. Neither approach leads to a distribution which shows a dip at $p_{ll} = 0$.

In the negative pion distribution in figure 22 one sees in addition a strong 'leading particle' effect, which comes from the identity of the produced particles with the incoming particle in this case. The effect gets less important as the multiplicity increases. We should also note that the slope of the exponential fall off is greater on the negative side of zero for both types of particle.

† p_{ll}, p_t and E are the single particle longitudinal and tranverse momenta and energy $E = m^2 + p_{ll}^2 + p_t^2$.

‡ This variable, also introduced by Feynman, has the following properties. Under Lorentz transformations along the collision axis it changes only by an additive amount so that distributions in y are Lorenz invariant. The invariant phase space element can be shown to be proportional to $dp_t^2\,dy$, so that there is no singularity at low energies.

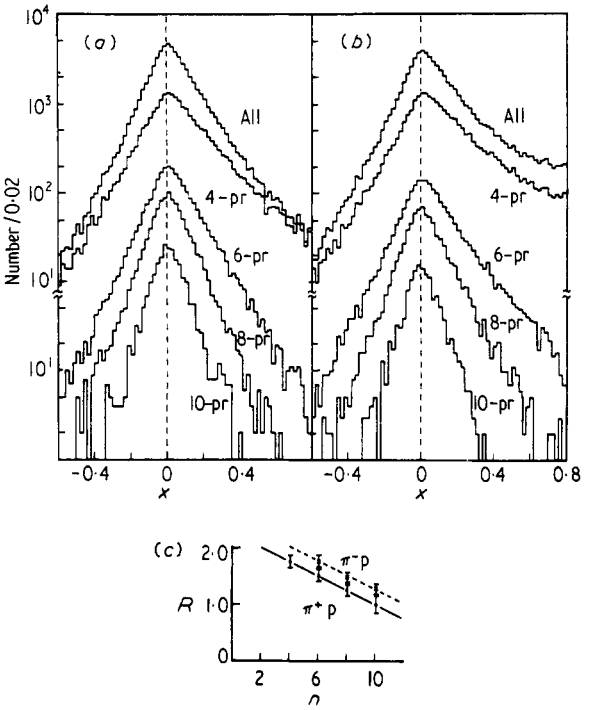

Figure 22. Distributions of Feynman's reduced longitudinal momentum variable x for the pions in (*a*) $\pi^+ p \to \pi^- +$ anything and (*b*) $\pi^- p \to \pi^- +$ anything at 18·3 GeV/*c*. (*c*) shows the ratio R of the proton to pion momentum which characterizes the symmetry frame of the produced pions (see § 12 of the text).

Similar distributions are found for single particles in proton–proton collisions. Kinsey *et al*† have studied pp interactions of 28·5 GeV and have tested the hypothesis that the distribution described by the invariant function $f(p_{11}, p_t)$ factorizes so that

$$\frac{d^2\sigma}{dp_t^2\, dp_{11}} = f_1(p_t) f_2(p_{11}).$$

The results do not support this suggestion. One might then wonder if the alternative factorization

$$\frac{d^2\sigma}{dp_t^2\, dp_{11}} = \frac{1}{E} g_1(p_t) g_2(p_{11})$$

which is not equivalent, since E is a function of both p_{11} and p_t, may be valid. This has also been tested by Biswas *et al* (1971) again with negative results.

A number of papers have tested the scaling hypothesis. A supercollaboration of groups studying positive and negative kaon interactions have compared the k^0 production in reactions $k^\pm + p \to k^0$ (or $\bar{k}^0$) + anything (Beupre 1971). The fraction of events leading to a neutral kaon, as a function of energy, is found to be constant at about 40%. Taken with the constant total cross section this implies a constant cross section for the inclusive reaction, and one which is approximately equal for k^+ and k^-. The distributions in the variable x are shown in figure 23. The agreement of the different energies is

† See Wroblewski (1970a).

excellent, but the k^+ and k^- differ appreciably. Note that here no account has been taken of the $1/E$ factor, so that this is not strictly Feynman scaling. It is early to reach conclusions about this but it seems possible that leading particles scale better without the energy factor, while the produced pions certainly need it.

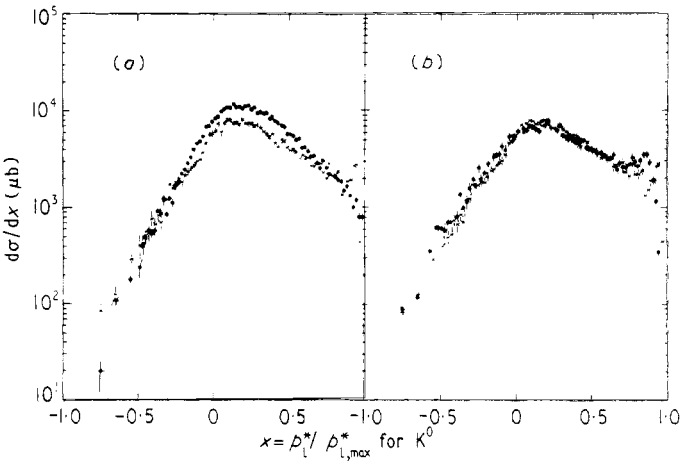

Figure 23. Distribution of the reduced longitudinal momentum for the K^0 in the reactions $K^+p \to K^0 + \text{anything}$ and $K^-p \to \bar{K}^0 + \text{anything}$. (*a*) ● $K^-p \to \bar{K}^0 + X^0$ at 10·1 GeV/*c*, × $K^+p \to K^0 + X^{++}$ at 8·2 GeV/*c*; (*b*) $K^+p \to K^0 + X^{++}$, ● 5 GeV/*c*, × 8·2 GeV/*c*.

Another interesting result of the kaon group is in the study of the effective mass distribution of 'anything' in the inclusive reaction. The ubiquitous exponential distribution appears again to give at least a first order description of the data, but this time a rising exponential with the mass. This result was quite unexpected by experimentalists, but does appear to have been a prediction of some thermodynamic models, and to be mainly a phase space effect. The data are shown in figure 24(*a*) and 24(*b*), this is broken down by multiplicity.

Finally in this section on inclusive reactions, figure 25 shows the variation with energy at a series of fixed values of x of the differential cross sections. The results have been derived by Chen *et al* (1971) from measurements by Anthony *et al*. Clearly the results give very good support for the scaling assumption for the produced pions, though they do not test it down to very low values of x.

We shall undoubtedly be hearing much more about experiments of this type in the months and years to come.

12. Symmetry frame for produced pions

It seems appropriate here to mention the work of Elbert *et al* (1971) on the inclusive reactions

$$\pi^- + p \to \pi^- + \text{anything}$$

and

$$\pi^- + p \to \pi^+ + \text{anything at 25 GeV/}c.$$

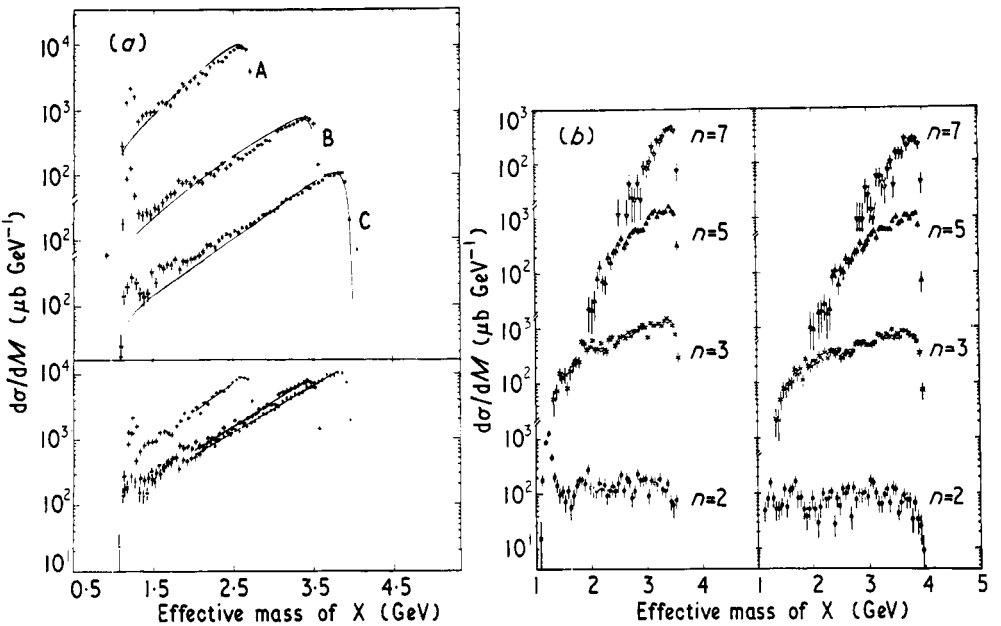

Figure 24. (*a*) The effective mass distribution for the system X in the inclusive reactions $K^{\pm}p \to K^0 + X$. A, $K^+p \to K^0 + X^{++}$ at 5 GeV/*c*; B, $K^+p \to K^0 + X^{++}$ at 8·2 GeV/*c*; C, $K^-p \to \bar{K}^0 + X^0$ at 10·1 GeV/*c*. (*b*) The same data broken down by multiplicity. The left hand side of (*b*) shows $K^+p \to K^0 + X^{++}$ at 8·2 GeV/*c*, while the right hand side shows $K^-p \to \bar{K}^0 + X^0$ at 10·1 GeV/*c*. The full curves in the upper half of (*a*) are phase space and in the lower half exponentials have been fitted to the data.

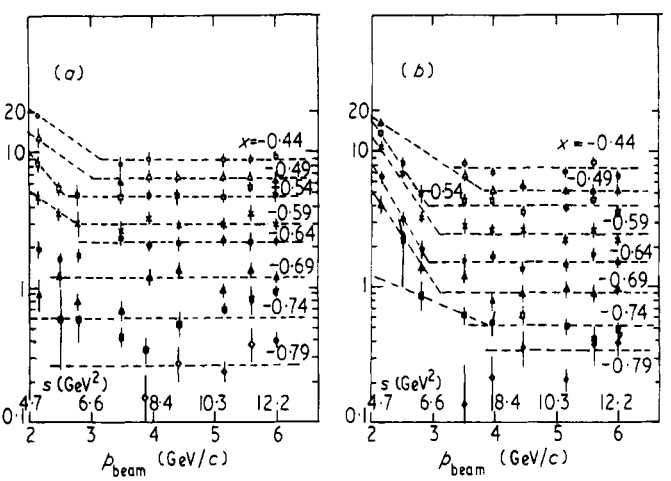

Figure 25. Scaling behaviour for the produced pions. The distributions, taken from Chen *et al* (1971), show the invariant function $f(x, p_t, s)$ evaluated for a series of fixed values of x and at $p_t = 0$, as a function of beam momentum. (*a*) $\pi^- p \to \pi^+ +$ anything; (*b*) $\pi^- + p \to \pi^- +$ anything.

To ensure that only produced pions were included, not contaminated with protons or the 'leading' negative pion positive pions were considered only in the forward, and negative ones only in the backward hemisphere. The longitudinal momentum distributions of the two types of particle are shown in figure 26. The data are fitted very well by

the form $\exp(-a|p_{11}|)$ for each set. However, the slope a is different in the forward and backward directions. That this should be so is not too surprising, since the colliding particles have different masses. However the authors hit on the idea of carrying out Lorenz transformations along the axis to find whether there exists a frame of reference in which the distribution is symmetric, and if so which it is. To test for symmetry they applied a chi-square test to the fit obtained assuming exponentials with equal slope. To define which frame of reference is being used they took the ratio R of the proton momentum to that of the pion. In figure 27 the chi-square probability is plotted against

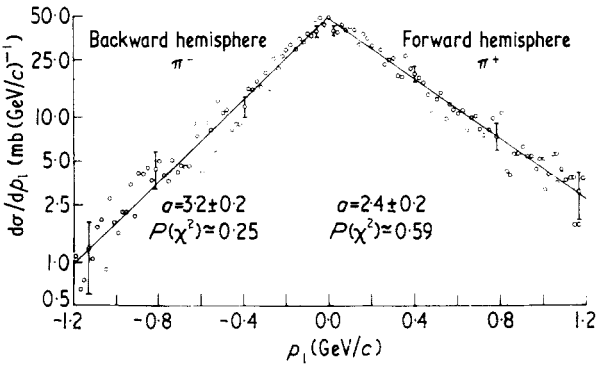

Figure 26. Longitudinal momentum distribution for the pions produced in the forward direction (π^+) and the backward direction (π^-) in $\pi^- p \rightarrow \pi^{\pm}$ + anything at 25 GeV/c. Data are from Erwin *et al* (1971).

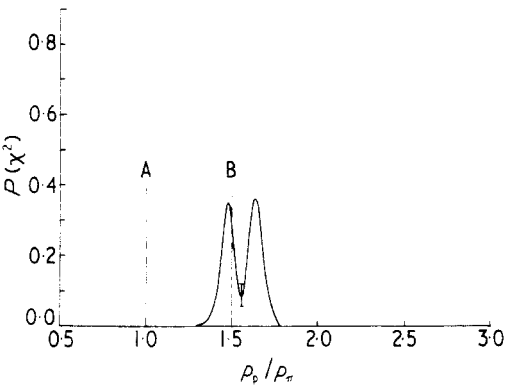

Figure 27. Search for a frame showing symmetry for the produced pions. The χ^2 probability for a symmetrical distribution of the type $\exp(-a|p_{11}|)$ is plotted against the ratio R of the incoming momenta of the proton and pions in the assumed reference frame. A, centre of mass system; B, quark system.

this ratio. It is found that symmetry exists in that frame in which the momentum ratio is 1·5. One intriguing possible explanation is that the collision is really between quarks, and that the symmetry frame is the quark–quark centre of mass. The meson production would then be envisaged to occur in some way such as that illustrated in figure 28.

A difficulty with this explanation is that the symmetry is only found in the quark frame when the mesons produced in all multiplicities are included; the results for different multiplicities are shown in figure 29 where it is seen that the ratio is strongly

multiplicity dependent. Biswas *et al* (1971) have also tested their data for a symmetry frame, and figure 22(*c*) shows the momenta ratio R, plotted against the multiplicities for π^+ and π^- interactions. Whether this must be taken as an indication against a quark explanation is not clear to the author.

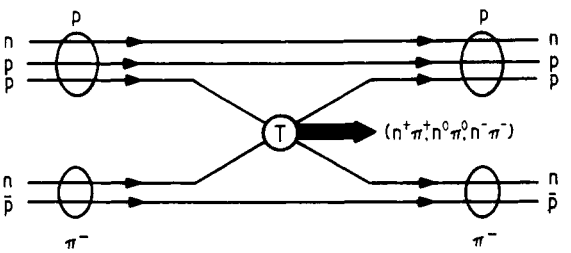

Figure 28. Schematic quark–quark collision.

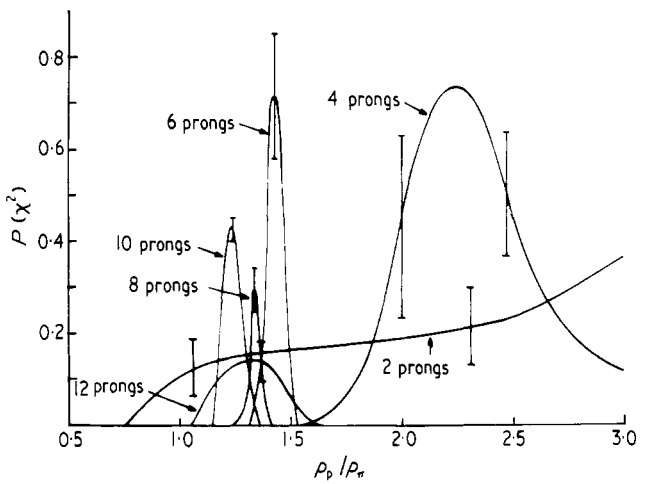

Figure 29. Search for the symmetry system in the data of figure 26 separated according to multiplicity.

13. Models for multiparticle states

We have seen in the preceding sections that the low transverse momenta and the behaviour of the cross section as a function of energy are strikingly suggestive of a multi-Regge pole exchange. Successful models for the amplitude must undoubtedly take this into account. However, we also know that there are resonances between particle pairs or larger groups of particles, which are due to poles in the amplitude. These poles are not present in the straightforward Regge pole exchange amplitude. Following the ideas of Dolen *et al* (1968) concerning the duality between resonances in any given channel, and Regge poles in the crossed channel, it is probable that the resonances are taken into account in some average sense in a Regge model. Developments of the Veneziano model to multiparticle states have permitted this feature to be included explicitly in an amplitude which has poles corresponding to resonances, and

shows Regge-like behaviour when the subsystem energies are large. In the following sections we shall discuss briefly the multi-Regge model and its developments, and then proceed to describe some of the features of the Veneziano model.

14. Multi-Regge model

In the pure multi-Regge model, it is assumed that the multiparticle final state is reached through a series of particle exchanges as illustrated in figure 30. The exchanged particles are assumed to belong to Regge trajectories, exactly as in a two particle scattering process. A further assumption is that the complete amplitude 'factorizes'. This means that it is a product of factors $s^{\alpha(t)}$ for each exchange, where $\alpha(t)$ is the appropriate Regge trajectory function, and factors to describe the couplings at the vertices.

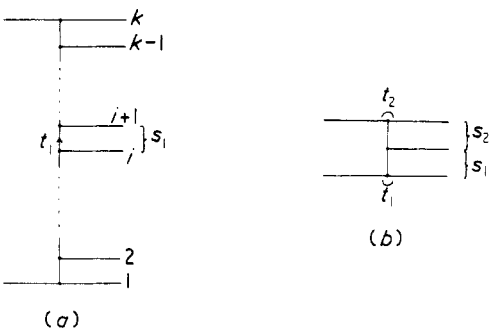

Figure 30. Regge ladder graphs for (*a*) general collision and (*b*) three-particle final state. The notation used in the multiperipheral Regge model is defined in this diagram.

Explicitly, if we consider the three-particle process illustrated in figure 30, the amplitude is written

$$T = cG_1(t_1)\left(\frac{s_1}{s_0}\right)^{\alpha_1(t_1)} G(t_1 t_2 \omega_{12})\left(\frac{s_2}{s_0}\right)^{\alpha_2(t_2)} G_2(t_2).$$

The functions G, which contain the Regge residue functions, are not fixed by the model, so it is usual to adopt exponential functions in order to obtain the peripheral behaviour observed in experiment. The quantity ω_{12} is an angle, concerned with the relative polarization of the Regge poles. As nothing is known about this, it is usual to neglect the dependence on this quantity; s_{10} and s_{20} are scale factors usually taken as 1 GeV^2.

The trajectory functions depend on the assumed exchanges. They are usually linear functions of the four-momentum transfer t written $\alpha(t) = \alpha_0 + \alpha' t$ where α_0 is the intercept of the trajectory, and α' its slope. For diffractive processes it is to assume a flat 'pomeron' trajectory with $\alpha_0 = 1$ and $\alpha' = 0$. This guarantees a constant cross section for a two body process which is produced by pomeron exchange.

In principle the Regge amplitude is supposed only to apply in the region where all the subsystem energies are large, so that for three particle states, only that region in

the centre of the Dalitz plot should be correctly represented. Experimentally, of course events are found to reside mainly near the edge of the plot, so that the Regge model describes only a small part of the data. Moreover, it is a property of the amplitude itself that it favours that part of phase space where one of the subsystem energies is large at the expense of the others. This is especially true if one exchange is a pomeron, when the large value of α makes the amplitude most important where the energy is shared so that all the other subsystem energies are small, which is precisely the diffractive effect which it is supposed to describe.

As a recent application of a pure Regge model, and one where it gave a very satisfactory description of the data, I would like to mention the work of Cho *et al* (1971) on the process $k^- + n \to k^- + \pi^- + p$ at 5·5 GeV/c. This channel is relatively free from resonances, so that the model appears to fit the data quite well without severe restrictions on the subsystem energies. Events were selected to give low four-momentum transfer to the nucleon but no other cuts were made in the data. The Van Hove LPS plot is shown in figure 31. There are two clear peaks, which can be seen to be associated with

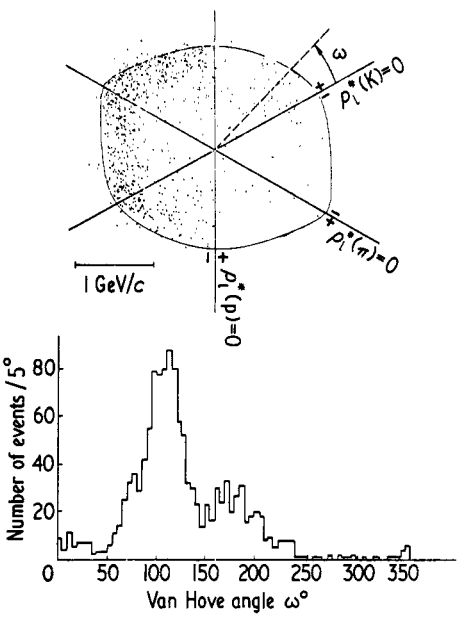

Figure 31. Van Hove LPS plot for the process $K^- + n \to K^-\pi^- p$ at 5·5 GeV. Data are from Cho *et al* (1971).

two dominant processes. These are the diffractive dissociation of the neutron ($\theta \simeq 100°$) and events where the negative pion is fast, and the kaon slow in the centre of mass system, which give $\theta \simeq 180°$. In the Regge exchange picture these must be due to exchange of the K* trajectory, with the pion at the top vertex. The authors assumed therefore pomeron/pion and K*/pion exchanges. They first selected the events from the LPS plot to give pure samples of each process and used these to fix the normalization of the two processes. They then added the two amplitudes and obtained a very fine fit to the overall data (figure 32). The diffractive contribution was about 60%.

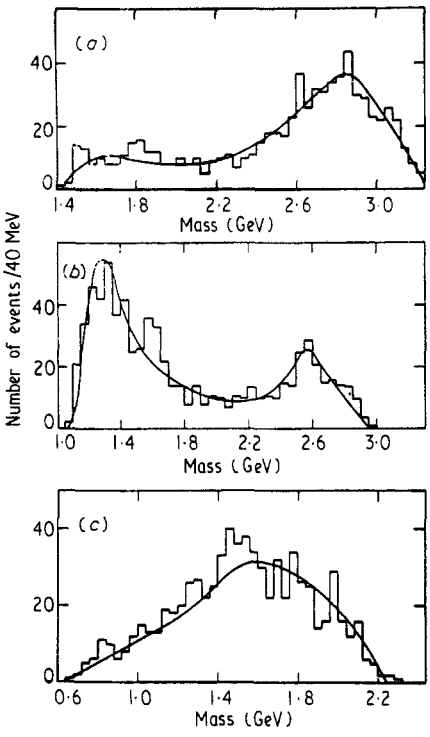

Figure 32. Effective mass plots for $K^-n \to K^-\pi^-p$ at 5·5 GeV fitted with the multi-Regge model. (*a*) K^-p; (*b*) π^-p; (*c*) $K^-\pi^-$.

15. Developments of the Regge model

The first reasonably successful attempt to provide an amplitude whose validity could be extended to the regions near the edge of the Dalitz plot was the model of Chan Hong-Mo *et al* (1968). This is a purely phenomenological model, with an amplitude chosen so that it is Regge-like when all the subsystem energies are large, but whenever one of the subsystem energies becomes small, the corresponding factor in the amplitude becomes constant, so that the behaviour follows phase space alone. Explicitly, the amplitude is written

$$|T| = \sum_{\text{permutations}} \prod_{i=1}^{n-1} \left(\frac{g_i s_i + ca}{s_i + a}\right)\left(\frac{s_i + a}{a}\right)^{\alpha_i}\left(\frac{s_i + b_i}{b_i}\right)^{\alpha_i}.$$

a, b, c, g are constants, which determine the energy at which the transition from phase space to Regge behaviour occurs, and the relative coupling strengths in two regions. The first success of this model was in explaining why there is a forward peak in the angular distribution of the Λ hyperons in kaon interactions which is absent in corresponding π meson proton processes. Essentially this is due to the possibility of pomeron exchange in the latter case, against which baryon exchange is unable to compete. For Λ production the baryon exchange must compete only with K meson or K* meson exchange, which allows baryon exchange effects to be more important. These results are shown in figure 33. However, the model has little physical content, and is not much

used in recent work. It does, however, still provide an amplitude which can be used to describe high-multiplicity interactions where the Veneziano model is impracticable, and, there being relatively little energy per particle, there is no region of phase space where all subsystem energies are large, so that a pure Regge model would not be appropriate anywhere†.

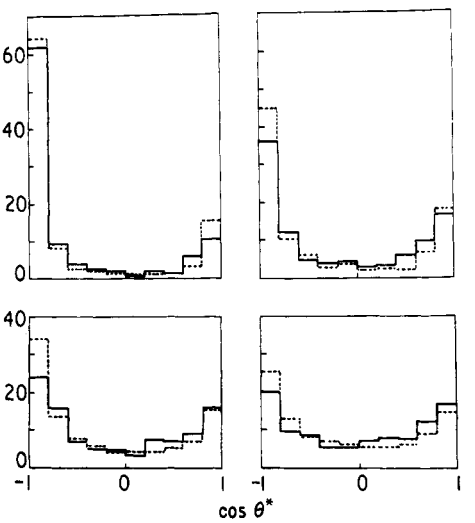

Figure 33. The angular distributions for Λ production in K^-p interactions, with the predictions of the CLA model. The forward peak, which develops with increasing multiplicity is due to baryon exchange graphs.

16. Veneziano model

It is not appropriate here to give a full account of the Veneziano model. However, before discussing its applications, a summary of some of its very beautiful features, which often seem quite close to the physical facts, seems appropriate. A fuller account can be found in articles by Chan Hong-Mo (1969) or by Jacob (1969).

In figure 34(*a*) we illustrate a scattering process between spinless particles. We know that the amplitude must have a series of poles in the variables s to give resonances in between particles a and b. These resonances should occur at values of s which are on the appropriate Regge trajectory, that is, for values of s such that $(\alpha_0 + \alpha' s)$ is a positive integer‡. α_0 is the intercept and α' the slope of the corresponding trajectory. To provide crossing symmetry, the amplitude must also have poles in the cross channel invariants t. These will occur at positive integer values of the t channel Regge trajectory: however, since for a physical scattering process t is always negative, these latter poles are not in the physical region. The remaining property required of the amplitude is that it must have Regge-like behaviour when s is large.

† An amplitude which permits the inclusion of resonances in the subsystems in a dual manner, has been proposed by Plahte and Roberts (1969) and may be a better phenomenological amplitude for high multiplicity reactions, in which resonances are important.

‡ We assume for simplicity here that the trajectories are exchange degenerate. For the general case when the trajectories must be given definite signature see the articles quoted (Chan Hong-Mo 1969, Jacob 1969).

Veneziano discovered that these properties are provided by the Euler β function, more often called B_4 in the present connection

$$B_4(-\alpha_s, -\alpha_t) = \frac{\Gamma(-\alpha_s)\Gamma(-\alpha_t)}{\Gamma(-\alpha_s-\alpha_t)}.$$

This has poles as required if α_s is a positive integer. It also has poles if α_t is a positive integer, but double poles are cancelled since if α_s and α_t are both integers there is also a pole in the denominator. It can also be shown that the function gives a Regge behaviour when s is large, so that it provides an explicitly dual amplitude. The remaining, and crucially important, feature is that the residue at the lth pole on the trajectory in the s channel is a polynomial of order l in the variable t. Now t is linearly dependent on the cosine of the scattering angle, so that the residue is a polynomial of order l in $\cos\theta$ also. This means that it describes mainly scattering by a resonance with angular momentum l, as required for the resonance on a Regge trajectory. (Note, however, that the polynomial is not precisely $P_l(\cos\theta)$, so that the resonance is not in a pure angular momentum state. There are resonances at the same energy in all the angular momentum states up to the lth. This is the well known phenomenon of 'daughters' which is probably a weakness of the model, though there are some cases, notably the ρ meson, where an s wave resonance which could be a daughter, does appear to exist. It is often called the ϵ.)

The extension of the Veneziano model to three and more particle final states became possible when a generalized beta function was developed by Bardakci and Ruegg (1968). The process $a+b \rightarrow c+d+e$ illustrated in figure 34 is now described by an amplitude which is a function of five independent variables, and the B_5 function is therefore written as a function of these variables. The variables chosen are the squared subenergies

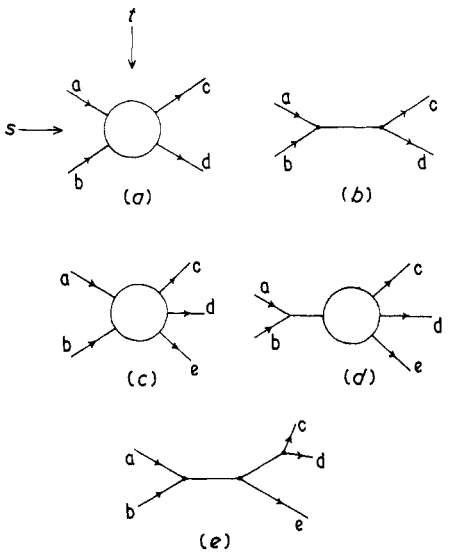

Figure 34. Schematic diagrams illustrating Veneziano four and five part functions. (*a*) Four point diagram; (*b*) pole expansion of the four point amplitude gives a Breit–Wigner amplitude corresponding to scattering through a resonant stage. (*c*) Five point diagram; (*d*) single pole corresponds to the formation of a resonance and its decay into three particles. (*e*) Double pole corresponds to the formation of a resonance followed by its decay into another resonance and a single particle, with subsequent decay of the second resonance.

between adjacent particles in the five-point graph $s_{i,i+1}$. As with B_4, there are poles in these variables, corresponding to resonance production, and the amplitude tends to Regge behaviour when the subsystem energies become large. The behaviour is thus just what we find experimentally. Again the lth pole along a trajectory has dominant behaviour corresponding to orbital angular momentum l, though daughter contributions are usually present.

The B_5 function as an amplitude to describe many-particle states has one additional feature, not relevant to the B_4 function. There exist double poles when two of the subsystem energies have simultaneously the appropriate values. If the subsystems both involve the same particle the double pole cancels in just the same way as in B_4. This means that all allowed tree-graphs such as in figure 34(*e*) are included. For example the formation of a resonance, followed by its decay into a second resonance and a stable particle, is correctly included. In fact, the residue at a pole is always a sum of B_4 functions; in particular near the first (s wave) pole in the variable s_{12} the B_5 amplitude can be approximated

$$B_5 \simeq \frac{1}{\alpha'(s_{12}-m_0^2)} B_4(-s_{34}, -s_{45}).$$

This can be interpreted as the formation of a resonance, with the pole term forming the Breit–Wigner and the B_4 describing the three-particle decay, or, if the pole is below threshold for a real process, the pole term is the Feynman propagator and the B_4 describes a virtual two-particle scattering process. It thus becomes possible to connect processes of different multiplicity. The process $a+b \to c+d+e$ can be related to the process $a+b \to c+z$ together with the coupling constant for the zde vertex†. This is illustrated in figure 35.

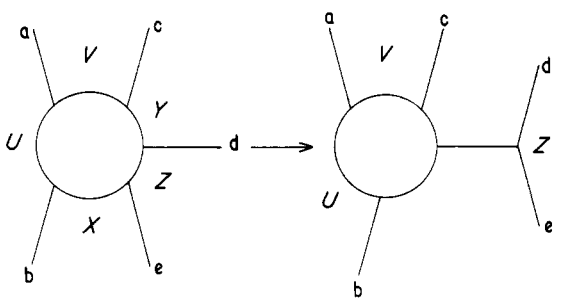

Figure 35. Illustrates the factorization property of the B_5 amplitude. The amplitude for the process $a+b \to c+d+e$ is described by a five-point function with trajectories U, V, X, Y, Z. By evaluating it at the pole corresponding to the particle Z, it is connected to the amplitude for the scattering $a+b \to c+z$, together with the Z coupling constant.

Further, because of the crossing symmetry of the amplitude, it is possible to connect some apparently quite separate physical processes with a common amplitude, and so fit a very large amount of physical data with a common analytic description. There are very few free parameters, though it is difficult to say precisely how many there are in a given calculation.

† This possibility, of course, is much more fundamental than the Veneziano model: it is assumed to be a feature of the pole structure of the amplitude T in general. However the Veneziano model gives an explicit analytic representation of T which permits the residues to be explicitly evaluated in terms of the values in the physical region.

In applications the trajectory functions to be used are chosen to provide the resonances experimentally observed. To this extent there is freedom in the model which amounts to putting in what one wants to find. However the trajectory parameters of all the main resonances are now well known, so that there is not much freedom to adjust these. Mixing diagrams with different permutations can cause cancellation of certain resonances, and this sometimes provides free parameters.

In its simple form, the Veneziano amplitude is a real scalar function, and the resonances are infinitely narrow. This is well known to violate unitarity, as well as being contrary to experience. It is usual to introduce a small imaginary part to the trajectory function to take care of the widths, which introduces some additional free parameters (and in fact spoils the factorization properties). When there is an odd number of pseudoscalar particles among the external legs of the process to be described, it is necessary that the amplitude should be pseudoscalar. This is usually arranged by introducing a pseudoscalar kinematic factor. For the three body final state this can only take the form $\epsilon_{\mu\nu\rho\sigma}p_1^\mu p_2^\nu p_3^\rho p_4^\sigma$ where ϵ is the Levi-Civita antisymmetric tensor, and the momenta are those of any four of the five external particles. This factor has itself very powerful effects on the angular and effective mass distributions, introducing angular momentum barrier effects, affecting the spin alignments of the resonances. While the effects are those observed, they are also a necessary feature of any realistic amplitude, satisfying parity conservation, and not unique to the Veneziano model.

A further weakness of the model is that it does not take account of the spin of the external particles. With bosons it is often possible to allow for spin by introducing a 'kinematic factor' though there appears to be no unique prescription for this. There is however no way at present of allowing for the spin of fermions, and it is usual to assume that the sum over spins will be sufficiently well represented by treating the particles as spinless. This is certainly a bad approximation, and since baryon trajectories do not show exchange degeneracy, and as there are not the restrictions on allowed exchanges from spin and parity and/or g parity which affect bosons, the model is very poorly defined for these cases. This has not prevented some very satisfactory applications, but it remains one of the reasons why, in its present form, it is difficult to take the model entirely seriously.

With these preliminary remarks, let us look at some of the results obtained. It is not possible here to give an extensive review†, but in order to emphasize how much data can be simultaneously described, I have taken a case which is 'classic' rather than very recent. This is the application by Chan Hong-Mo *et al* (1970) to the three processes

$$k^+ + p \to k^0 + \pi^+ + p$$
$$k^- + p \to \bar{k}^0 + \pi^- + p$$
$$\pi^- + p \to k^0 + k^- + p.$$

Through application of crossing symmetry and isotopic spin invariance these three processes can be described by a common amplitude, and there is really only one free parameter. The plots on figures 36 and 37 show the fit to all three channels—figure 38 shows some resonance decay angular distributions, fitted with the amplitude. These angular distributions are, however, a consequence of the pseudoscalar kinematic factor and not of the Vereziano amplitude itself. By using further the technique described

† A rather complete review of applications of the Veneziano five point amplitude to three-body final states has been given by Schreiber (1971).

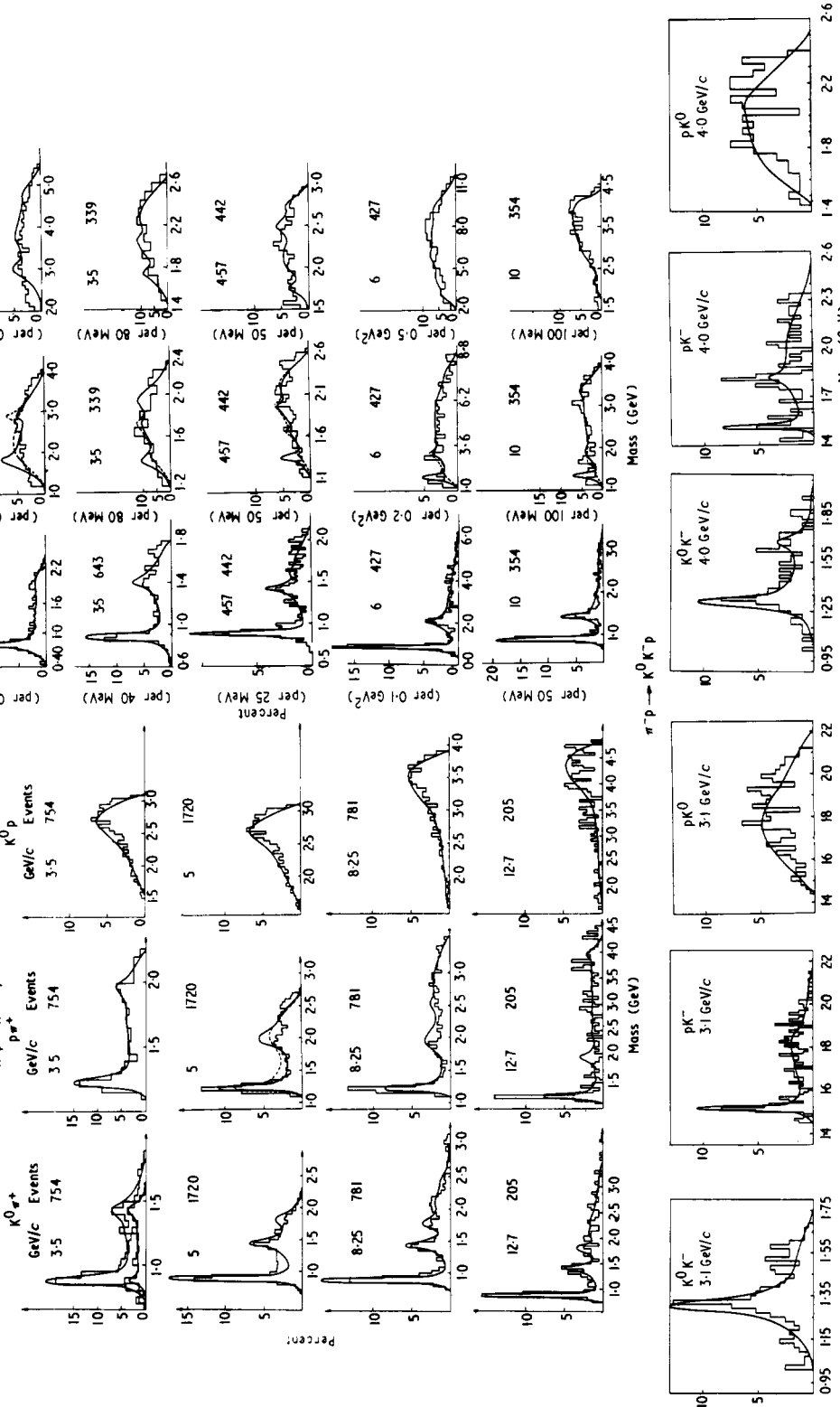

Figure 36. Effective mass distributions for three different processes at several energies described by a single amplitude (from Chan Hong-Mo 1970), with one free parameter.

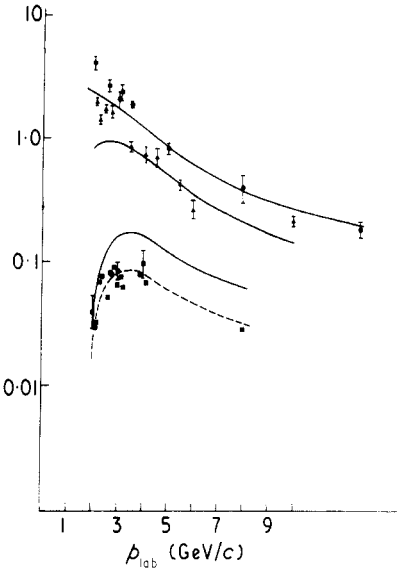

Figure 37. Total cross sections for the three processes illustrated in figure 36 fitted with a common amplitude. Agreement for the third process is out by a factor of about 2, but the shape is right. ● $K^+p \rightarrow K^0\pi^+p$; ▲ $K^-p \rightarrow \bar{K}^0\pi^-p$; ■ $\pi^-p \rightarrow K^0K^-p$.

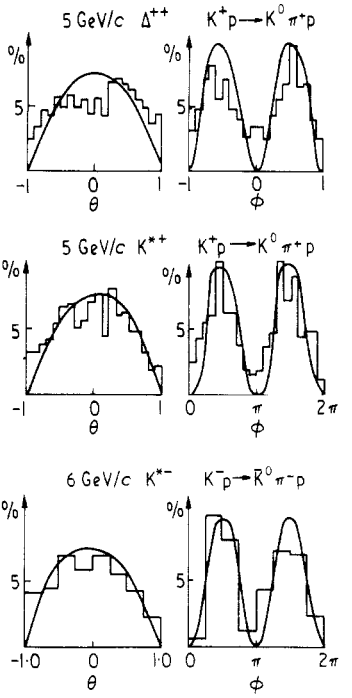

Figure 38. Resonance decay angular distributions for the processes indicated. Full curves are the predictions of the eight-point amplitude used by Chan Hong-Mo (1970).

above of connecting the five point amplitude to the four point function which is the residue at the leading pole, Peterson and Thomas (1970) have evaluated the predictions of the model for the following four processes with no further parameters:

$$k^- p \to \bar{k}^0 n \qquad \pi^- p \to k^0 \Lambda^0$$
$$k^+ n \to k^0 p \qquad k^- n \to \pi^- \Lambda.$$

The comparison with experiment for the total cross sections is shown in figure 39. The agreement in all these cases is really remarkably good. There is no doubt that the description, albeit rather rough, of so much data, representing the amplitude in unconnected regions of the complex parameter space, and involving quite distant analytic continuations of the amplitude, represents a degree of success which cannot be taken lightly.

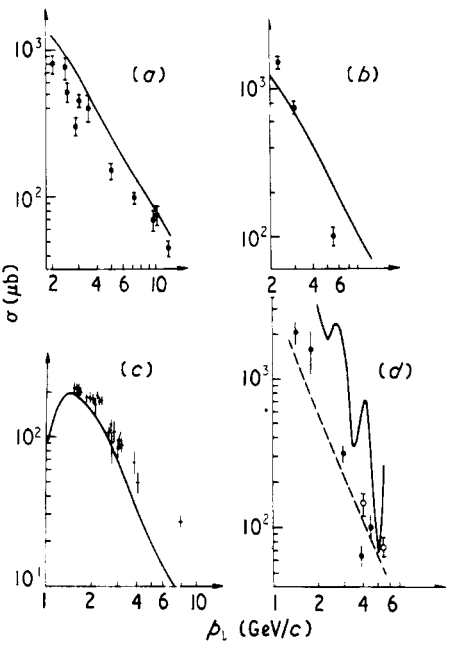

Figure 39. Total cross sections for two-body processes related to the three processes illustrated in figures 37 and 38 by factorization. The full curves are the calculations of Peterson and Thomas (1970) using the amplitude of Chan Hong-Mo (1970) with no additional parameters. (*a*) $K^- p \to \bar{K}^0 n$; (*b*) $K^+ n \to K^0 p$; (*c*) $\pi^- p \to K^0 \Lambda^0$; (*d*) $K^- n \to \pi^- \Lambda$.

17. Dual diffractive models

For reasons that go beyond the limits of this review, the Veneziano model can be applied only with linear rising trajectories. This means that it is incapable of describing processes where the pomeron contributes. If, however, we assume that the pomeron exchange can be factorized as if it were a pole term, we should be able to write for a dissociation process illustrated in figure 40 which also defines the notation

$$T = F_1(t_{pp}) s F_2(s_{bc}, t_{ab}).$$

The function F_1 is a form factor for the proton, and F_2 is the description of the dynamics

of the excited 'fireball'. s is the 'propagator' for the pomeron; if we assume a normal Regge description we shall use s^{α} where α, being the trajectory function for the flat pomeron is just 1. For the top vertex it is appealing to take a Veneziano form, since this gives a simultaneous description of the resonance production by pomeron exchange, and the Deck processes described earlier. A model of this type was used by Pokorski and Satz (1970) to describe the dissociation of the nucleon, F_2 being a suitably chosen combination of B_4 terms. The results, shown in figure 41 are quite pleasing. However,

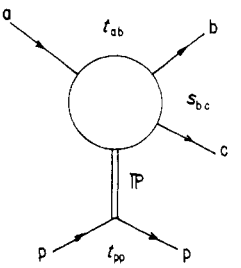

Figure 40. The dual diffractive model of Pokorski and Satz (1970).

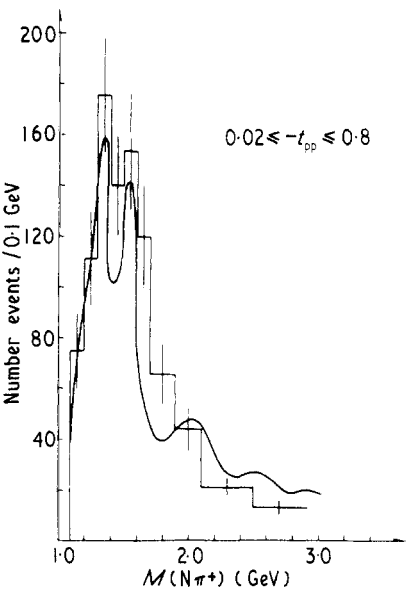

Figure 41. Predicted effective mass plot for nucleon dissociation compared with results for $pp \rightarrow pn\pi^+$ according to the model of Pokorski and Satz.

they suffer from the difficulties always associated with baryon trajectories in the Veneziano model. Dissociation of a pseudoscalar meson into two particles by diffraction is not possible if we assume the pomeron to behave like a 0^+ particle. To describe the diffractive dissociation of the k meson, Bartsch *et al* (1970a) used a B_5 amplitude at the upper vertex. The predictions of the calculation include a description of the Q and L mesons as Regge recurrences of the kaon, and a description of the decay of these objects in terms of the distributions on the Dalitz plot which seem remarkably

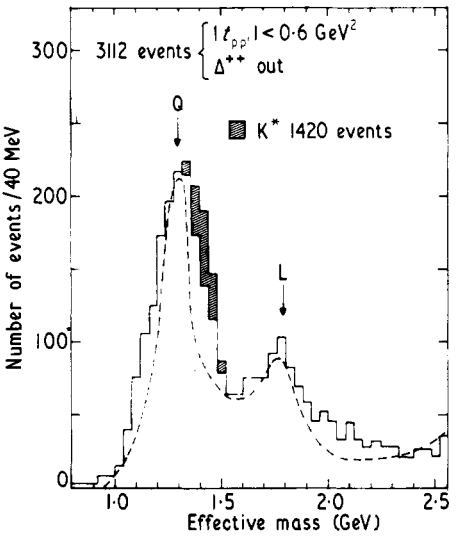

Figure 42. Effective mass plot for the (Kππ) system in $K^-p \rightarrow (K^-\pi^+\pi^-)p$ at 10 GeV/c. The broken curve shows the predictions of the dual diffractive model (Bartsch *et al* 1970a). Q and L represent the positions of the resonances known by these names.

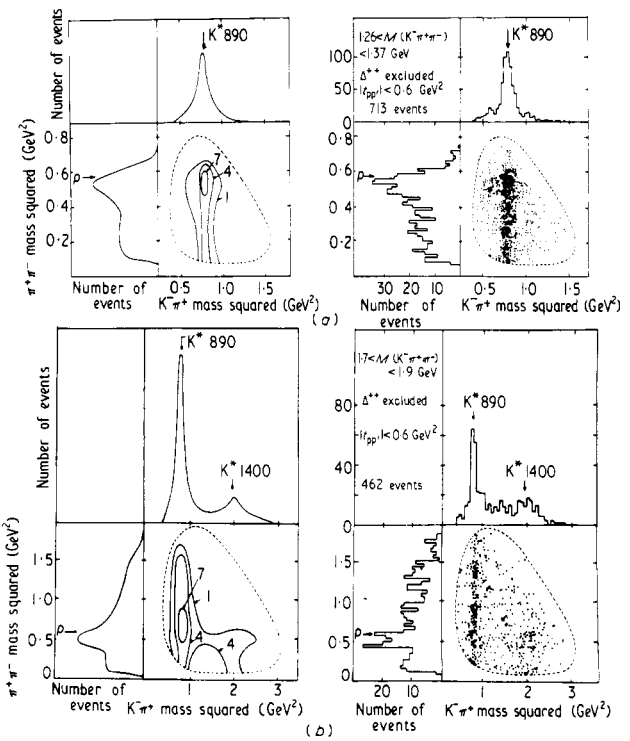

Figure 43. Dalitz plot distributions for (*a*) the Q region and (*b*) the L region using the dual diffractive model (Bartsch *et al* 1970a). The left hand sides of each are the predicted and the right hand sides the experimental plots.

good. These results are reproduced on figures 42 and 43. A similar description of the pion dissociation has been given by Hirschfield and Shah (1970).

The description of nucleon dissociation into a nucleon and pion given by the Pokorski–Satz model offers a means of describing the pomeron contributions to the processes such as $k^{\pm}+p \rightarrow k^{\pm}+\pi^0+p$, or $k^{\pm}+\pi^{+}+n$. In these cases, at the energies achieved so far, the pomeron effects are appreciable but not dominant, as we saw in §§ 8 to 10. There have been two attempts to combine a diffractive amplitude obtained from the Pokorski–Satz model with a conventional B_5 amplitude, so as to get a correct overall description of the channel. The estimates of the fraction of each amplitude required give the relative importance of the pomeron contribution as between 25 and 50% in the 10 GeV/c region. Figure 44 shows the calculation of Kajanti and

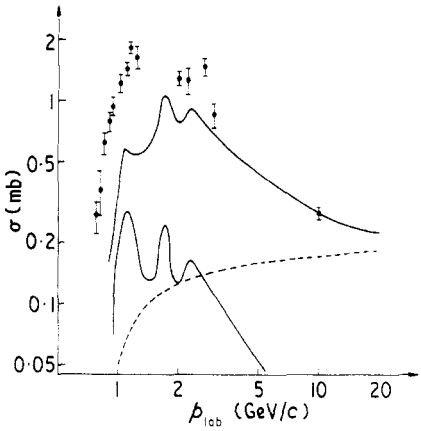

Figure 44. The calculations of Kajanti and Papagiorgiou. The lower curve is the prediction of the B_5 amplitude chosen to describe $K^-p \rightarrow K^-\pi^0p$. The broken curve is the prediction of the dual diffractive model with pomeron exchange. The combined cross section is the upper full curve.

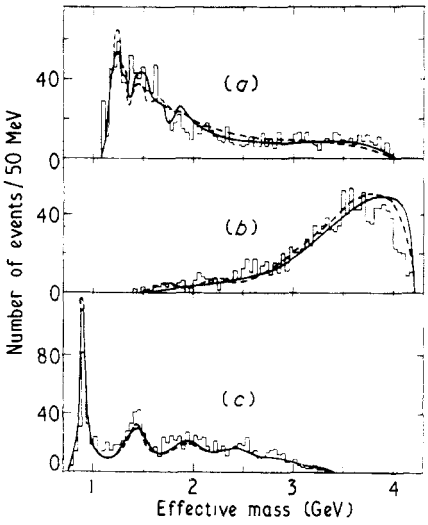

Figure 45. Calculation similar to that shown in figure 44 (from Bartsch *et al* 1970b) for the case $K^-p \rightarrow nK^-\pi^+$. The curves are effective mass distributions for (*a*) $n\pi^+$: (*b*) nK^- and (*c*) $K^-\pi^+$.

Papagiorgiou (1970), showing how the cross section is built up of pomeron exchange and dual parts. The other similar calculation (Bartsch *et al* 1970b) is illustrated in figure 45.

18. Conclusion

We have reviewed briefly a wide range of results on multiparticle states. It is evident that these complex processes are not yet fully understood and present many interesting problems. However, considerable progress has been made in recent years in providing a reasonable phenomenological description of many important features. To keep the article of reasonable size the work of many authors has been left out, and no discussion has been included of thermodynamic models or other statistical models of hadron dynamics, which form a large enough topic for a review of their own.

References

Anzon E V *et al* 1970 *Phys. Lett.* **31B** 237–40
Bardakci K and Ruegg H 1968 *Phys. Lett.* **28B** 342–7
Bartsch J *et al* 1970a *Nucl. Phys.* B **24** 221–30
Bartsch J *et al* 1970b *Nucl. Phys.* B **23** 1–18
Bartsch J *et al* 1970c *Nucl. Phys.* B **19** 381–98
Beneke J, Chou T T, Yang C N and Yen E 1969 *Phys. Rev.* **188** 2159–69
Beupre J V *et al* 1971 *Nucl. Phys.* **830** 381–97
Biswas N N *et al* 1971 *Phys. Rev. Lett.* **26** 1589–92
Boesebeck K *et al* 1971 *Nucl. Phys.* B **28** 381–96
Chan Hong-Mo 1969 *CERN TH* 1057
Chan Hong-Mo, Hsue C S, Quigg C and Wang J M 1971 *Phys. Rev. Lett.* **26** 672–4
Chan Hong-Mo, Loskiewicz J and Allison W W M 1968 *Nuovo Cim.* A **57** 93–120
Chan Hong-Mo, Raito R O, Thomas G H and Tornqvist N A 1970 *Nucl. Phys.* B **19** 173–98
Chen M, Ling-Lie Wang and Wong T F 1971 *Phys. Rev. Lett.* **26** 280–3
Chew G F and Pignotti A 1968 *Phys. Rev.* **176** 2112–9
Cho Y *et al* 1971 *Phys. Rev.* D **3** 1561–8
Dolen R, Horn D and Schmidt C 1968 *Phys. Rev.* **166** 1768–81
Elbert J W, Erwin A R and Walker W D 1971 *Phys. Rev.* D **3** 2042–7
Feynman R D 1969 *Phys. Rev. Lett.* **23** 1415–7
Flaminio E, Hansen J D, Morrison D R O and Tovey N 1970 *CERN/HERA* 70-6
Goldsack S J *et al* 1971 *Nucl. Phys.* B **29** 529–46
Hansen J D, Kittel W and Morrison D R O 1970 *CERN/D Ph II/Phys.* 70-32
Hirshfeld A C and Shah 1970 *University of Heidelberg Preprint*
Hofmokl T and Wroblewski A 1970 *Phys. Lett.* **31B** 391–3
Honecker R *et al* 1971 *Nucl. Phys.* **32** 141–8
Jacob M 1969 *CERN Th* 1020
Jones L W *et al* 1970 *Phys. Rev. Lett.* **25** 1679–86
Kajanti K and Papagiorgiou S 1970 *Nucl. Phys.* B **22** 31–44
Kittel W, Ratti S and Van Hove L 1971 *Nucl. Phys.* B **30** 333–73
Mueller A H 1970 *Phys. Rev.* D **2** 2963–8
Muirhead H and Poppleton A 1969 *Phys. Lett.* **29B** 448–50
Peterson B and Thomas G H 1970 *Nucl. Phys.* B **20** 451–60
Plahte E and Roberts R G 1969 *Lett. Nuovo Cim.* **1** 187–91
Pokorski S and Satz H 1970 *Nucl. Phys.* B **19** 113–24
Rinaudo G *et al* 1971 *Nucl. Phys.* B **25** 351–73
Rotelli P 1969 *Phys. Rev.* **182** 1622–7

Schreiber H J 1971 *Deutsch. Akad. Wiss., Berlin Phe* 71-5
Van Hove L 1969 *Nucl. Phys.* B **9** 331–48
Wang C P 1969 *Phys. Rev.* **180** 1463–7
Wroblewski A 1970a *Proc. 15th Int. Conf. on High Energy Phys., Kiev* to be published
—— 1970b *Phys. Lett.* **32B** 145–8